NATURAL FREQUENCIES OF COMPOSITE BEAMS WITH FLAWS

A Thesis Submitted
In Partial Fulfilment of the Requirements
for the Degree of

MASTER OF TECHNOLOGY

by

J. P. PARIKH

to the

DEPARTMENT OF AERONUTICAL ENGINEERING

INDIAN INSTITUTE OF TECHNOLOGY, KANPUR

MAY, 1983

CERTIFICATE

This is to certify that the work "NATURAL FREQUENCIES OF COMPOSITE BEAMS WITH FLAWS" has been carried out under our supervision and has not been submitted elsewhere for a degree.

(N.G.R. IYENGAR)
Professor
Department of Aero. Engg.
I.I.T. Kanpur

(P.N. MURTHY)
Professor
Department of Aero.
I.I.T. Kanpur

ACKNOWLEDGEMENTS

I express my heart felt gratitude to Professor P.N. Murthy and Professor N.G.R. Iyengar for their invaluable guidance and keen interest throughout the course of this work.

I am indebted to Professor B.D. Agarwal and Dr. D. Yadav for their kind help and discussions.

I am thankful to Mr. Lalit Gupta, Mr. R.K. Nakrani and Mr. B.S. Patro for their considerable help and interest during fabrication and testing.

I take this opportunity to thank Mr. C.K. Awasthi who made my stay a pleasant one by rendering a helping hand whenever needed.

I acknowledge with thanks the help provided by Mr. J.R. Umaretiya, Mr. Dinesh Jain and Mr. Deepak Shah.

I thank Mr. S.K. Tiwari for his excellent typing and Mrs. Shanti for her fine cyclostyling.

CONTENTS

LIST OF TABLES

LIST OF FIGURES

LIST OF SYMBOLS

Symbol	Meaning
$[D]$	Bending stiffness matrix
$\{\delta\}^{(e)}$	element displacement
E_L, E_T	Elastic constants in longitudinal and transverse directions
$[K]$	assembled stiffness matrix
$[K]^{(e)}$	element stiffness matrix
L_1, L_2, L_3 & L_4	volume coordinate
L	length of the beam
$[M]$	assembled mass matrix
$[m]^{(e)}$	element mass matrix
N_1, N_2, N_3, N_4	shape functions at each node of tetrahedra
Q_{ij}	reduced stiffnesses
$\bar{Q}_{ij}$	Transformed reduced stiffness
$\{\delta\}$	vector of global displacements
ρ	mass per unit length of beam
T	Kinetic energy
$[T]$	Transformation matrix
U	strain energy
u	displacement in X direction
v	displacement in Y direction
V	volume
ω	circular frequency

w	displacement in Z direction
$\lfloor W \rfloor$	displacement distribution along the element
X	global cartesian coordinate
Y	global cartesian coordinate
Z	global cartesian coordinate
	eigen value parameter
$\epsilon_x, \epsilon_y, \epsilon_z$	strain components in XY plane
θ	fiber orientation
ν_{LT}, ν_{TL}	Poisson's ratio in longitudinal & transverse directions respectively

ABSTRACT

This thesis reports the investigations carried out to find the effect of flaws in laminated composite beams on natural frequencies. Laminated composite beams with and without flaws are fabricated using hand lay up techniques. Finite element formulation is eomployed to determine the natural frequencies, theoretically. The subdivision of space volume into individual tetrahedral, sometimes, presents difficulty in visualization. A more convenient subdivision of the structure is found to be eight cornered brick elements. A brick element can be divided into five tetrahedra. Theoretical and experimental results are presented in tabular and graphical forms. Beams with simply supported and clamped-clamped boundary conditions are investigated. It is observed that natural frequency decreases with increase of flaw area, length and for fiber orientations from 0° to 90°. It is observed that delamination for cross ply is predominant as the flaw area increases.

CHAPTER - 1

INTRODUCTION AND LITERATURE REVIEW

1.1 INTRODUCTION :-

Any material having two or more distinct constituents or phases and having properties noticeably different from properties of its constituents is considered as a "Composite Material". A composite with fiber as one of its constituents is called fiber-reinforced composite and is one of the earliest and most widely used. In fiber-reinforced composite the strength, stiffness and other properties in different directions can be easily tailored to our needs by changing constituent materials, fiber orientation, stacking sequence and other manufacturing variables. The potential use of fiber composites in developing light weight applications with high strength engineering material is now well recognized.

The structural design using the fiber-reinforced plastic (FRP), requires the characterization of their behaviour under static and dynamic loading conditions because it is expected that the behaviour of the composites will be different under two loading conditions.

Laminated plate forms an important structural element in the design of aerospace, mechanical, automobile and other structural applications. Advanced composite materials

offer a significant potential for reducing the weight of aircraft structural members for both primary and secondary load carrying members. Examples of laminated composites include aerospace vehicles, missile cases, aircraft wing panels and body sections, rocket motors, rotor blade of a modern helicopter, large wind generator, fiber-glass boat hulls tennis rackets, nose gear doors, engine nacellels and control surfaces, rotor blade trailing edge, horizontal and verticle stablizers, gear box etc.

The recent investigation reported by Gunnik et al (1) and Wicker (2) of a new hybrid material is obtained by the adhesive bonding of a number of thin aluminium alloy sheets and aramid layers to produce an aramid reinforced aluminium laminate(ARALL). Application of ARALL in aircraft structure can lead to large weight savings, especially where fatigue and damage tolerance are important design criteria. Well known examples are wing tension skins, and pressure cabins of transport aircrafts. ARALL shows very favourable fatigue crack growth properties and has a high tensile yield strength. Also fatigue test on lugs, centrally cracked specimens, and bolted and riveted joint specimens show highly superior fatigue properties in all cases for ARALL, as compared with aluminium alloys when fatigue is a significant design criterion in setting allowable stress levels, preliminary design on a wing tension skin and on fuselage skins of

different types of aircraft indicates a weight saving for wing skin of more than 30 percent and for fuselage skins from 20 to 50 percents.

With the increasing use of composite materials, a need has been created for unique repair methods for millitary and commerical aircrafts which include boron/epoxy, graphite/epoxy, fiber glass/epoxy and Kevlar/epoxy. Repairs to composite materials are intended to restore the strength of the part to at least 100 percent of its original strength. The allowable size of the field repairs is often limited.

Patches can be applied in the form of surface stepped, or scarf. Stepped and scarf patches have the advantage of providing a smoother surface than surface patches. However, because of difficulties in machining the aircraft parts for these patches (stepped or scarf), surface patches are most commonly used.

Laminated composites are fabricated by, either hand lay-up technique, or using moulds, or the filament winding machine. The laminated composites are fabricated at room temperature as well as at a high temperature. Composites fabricated by any type of these techniques will result in flaws, which would be of micro or macro level. This appears in the form of blow holes or some foreign materials within a lamina or between two laminae. The strength of the laminated mainly depend on shape, size and location of these

flaws. If flaws of sufficient sizes are present at the interface of the lamina, it may lead to delamination.

A great deal of current research, both analytical and experimental, is therefore, being directed towards understanding the behaviour of these materials in the presence of flaws. In what follows, the relevant literature is reviewed.

1.2 LITERATURE REVIEW :-

The analysis of natural frequency of vibration, deflection and strength due to action of lateral loads has become increasingly important with the advent of highly anisotropic fiber-reinforced composites.

Kulkarni and Frederick (3) have studied the effect of delamination in laminated composite cylinders for different axial and circumferential wave numbers. For lower axial wave numbers, the difference in the frequencies, is negligible. The departure in the frequency increases with an increase in circumferential wave number. They have observed the distinct difference for m=1 and n=10 (304 cps), where m is axial wave number and n is circumferential wave number. But for m=3 and n=10 the difference is only 72 cps. Further, for high values of n, increased m has a restoring effect. This restoring effect will also depend on the location of unbonding.

Daniel (4) has presented the results of experimental investigation of deformation and failure of $[0°/\pm 45°/90°]$ lay up of graphite epoxy laminates with circular holes subjected to an equal biaxial tension. Failure and delamination at 22° to the fiber axis and maximum strains on the hole boundary reach twice the values for unnotched laminates.

Stepanenko et al (5) deal with bonding of structures of composite materials under the assumption that internal energy in the material is an important factor in the reduction of vibration of structures. Theoretical and experimental results for rods of different bondings show dependence, of the logarithmic vibration decrement, endurance limit and dynamic strength of material, on the angular orientation.

Harris and Orringer (6) have determined the interlaminar tension by using a delamination coupon in which the tension component is predominant. By a simple argument, it is concluded that middle plies should be at 90° while the outer one may have a $\pm \theta$ sequence. Thickness and number of plies in each orientation are designed to maximize the interlaminae tension and minimize shear. By conducting tests on specimens with stacking sequence $[(\pm \theta)_2 / 90]_s$ and $[\theta/(-\theta)_2/\theta/90]_s$, it is found that delamination starts at 0/90 interface instead of 90/90 midplane concluding that failure was due to combined stress (but not pure tension).

Chawla et al (7) have conducted tension fatigue tests on notched specimens and reported on crack characteristics of 30 percent stainless steel and 70 percent aluminium laminates. It was observed that crack growths in laminates were found to be lower than those in conventional metals.

Glavotto et al (8) has studied a formulation of the problem for calculation of the stiffness and stresses of beam sections made of anisotropic and non-homogeneous materials such as the rotor blades of a modern helicopter or of a large wind generator. Heterogeneity can cause conditions of 3-Dimensional stress (which can also include significant interlaminar stress) which are not found in homogeneous beams where the method allows the solution of a bidimensional problem which discretized by the finite element technique, can be reduced to a set of simultaneous algebric equation in the central zones and to the research of the eigen solution of a matrix polynomial in the terminal zones.

Tirosh et al (9) have carried out an investigation by considering a single fiber in an infinite elastic body with a crack and concluded that lowest transverse strength is obtained for the case of circumferential microcracks near the interface. Also, the reduction of fiber diameter minimizes the weakening of the matrix.

Ahmed (10) has studied the flexural vibration characteristics of curved sandwitch beams. 3-Dimensional models are used incorporating an element having 3,4 and 5 degrees of freedom per node and various parametric studies are made to investigate their effect on the natural frequencies of curved clamped-clamped sandwitch beams.

Singh (11) has studied the effect of flaws, on laminated composite beams with one edge free and the other edge clamped. The solution of the governing differential equation was obtained by using finite difference theory. He observed that :

(1) first natural frequency decreases monotonically when fiber orientation increases from 0° to 90°. The effect of flaws are found to be important for small fiber orientations.

(2) decrement in natural frequency increases with increase in flaw area.

(3) first natural frequency increases with an increase in the length of the specimen, also the effect of flaws, in reducing natural frequency is more for smaller lengths.

(4) effect of flaws, in reducing the first natural frequency increases as flaw from structural reference axis move towards top or bottom surface of the specimen.

(5) decrement in natural frequency is maximum when flaw is near the root and is negligible near the tip.

An attempt is made in this thesis to extend the work of Singh (11) to include other boundary conditions. Further, it is well known that in a laminated structure, it is not always possible to obtain closed form solutions. Keeping this in mind and the fact that the presence of flaw changes the characteristics locally it becomes imperative to look for techniques which can take into account these effects as accurately as possible.

The finite element technique which has been well proven for a variety of problems, is employed here to model the structural behaviour.

Chapter 2 deals with theoretical analysis of laminated composite beams using a finite element technique.

The experimental technique and the set-up are discussed in Chapter 3.

The results of the investigation are discussed in Chapter 4, along with the suggestions for further work in this direction.

CHAPTER - 2

FINITE ELEMENT FORMULATION

2.1 INTRODUCTION :-

The finite element method which takes into account all the possible variations in strength etc., is found to be suitable for a theoritical investigation of this problem. In composite beam the strength of each lamina is different because of fiber orientation and thickness. This results in a change in stresses at each lamina. Though the structure is basically two dimensional the presence of flaw reduces the behaviour as that in three dimensional structures.

In the finite element method, the structure is divided into a number of subdomains or elements in terms of matrices, e.g. elastic stiffness and inertia matrices in the case of a dynamic problem. These matrices are evaluated by invoking the variational principle.

The finite element method applied to continuum is very similar to that applied to discrete structural systems. The main difference lies in the fact that the continuum is first idealized as a conglomeration of elements and the forces acting on the element are idealized into nodal forces. Either force method or the displacement method is proposed to be used.

In what follows, we shall discuss the salient features of the finite element technique.

Step (1) : Structure is idealized into a number of finite elements.

Step (2) : Forces acting on each of the element are lumped at the nodal points.

Step (3) : Each element is described in terms of local coordinate system and the relation between the nodal forces and deformations of the element are obtained using stress-strain relation of the material. A displacement function is assumed such that the geometric compatibility at the interface of the adjacent elements is satisfied as far as possible. The relation between the nodal forces, nodal displacement and the external loads acting on the element is developed from the virtual work concept. In isotropic analysis the stresses change from point to point but in laminated composite the stresses change from layer to layer for different orientations and thickness of each lamina.

Step (4) : Equilibrium of each of the nodes is satisfied by considering the forces acting at the corresponding nodes of elements connected to a point.

The above steps are valid for static as well as dynamic problems. However the variation principle corresponding to a dynamic problem is the Hamilton principle.

2.2 VIBRATION PROBLEM :-

The vibration problem can be formulated using the stationary property of the lagrangian as,

$$\delta (U-T) = 0 \qquad \text{---------------} \quad (1)$$

where, U is the strain energy and T is the kinetic energy.

In the finite element analysis U and T can be written as [12]

$$U=\tfrac{1}{2} \{\rho\}^T [K] \{\rho\} \qquad \text{-----------} \quad (2)$$

and

$$T=\tfrac{1}{2} \omega^2 \{\rho\}^T [M] \{\rho\} \qquad \text{---------------} \quad (3)$$

where $[K]$ and $[M]$ are the stiffness and the mass matrices of the entire structure, $\{\rho\}$ is the vector of global displacements and ω is the circular frequency. The matrices $[K]$ and $[M]$ are "assembled" from the element stiffness matrix $[k^{(e)}]$ and element mass matrix $[m^{(e)}]$.

Substituting U and T in Eqn. 1 and taking the variation we obtain,

$$[K]\{\rho\} - \omega^2 [M]\{\rho\} = 0 \qquad \text{---------------} \quad (4)$$

which is the governing equation for free vibration of a structure. The frequency w and the $\{\rho\}$ vector of global displacement can be obtained by an algorithm called "simultaneous iteration algorithm for symmetric eigen value problems" after obtaining $[K]$ and $[M]$ for the elastic structure.

2.3 CHOICE OF THE ELEMENT :-

The nodal points are specified by three global cartesian coordinates X, Y and Z. Three degrees of displacements u, v, w along X,Y and Z result in 12 degrees of freedom for each element.

The division of a space volume into individual tetrahedral, sometimes, presents difficulties of visualization and could easily lead to errors in nodal numbering etc. However, the input of the elements is given as either 8 nodal brick elements or 6 nodal tetrahedral as shown in Fig. 2.1.

A more convenient subdivision of the structure is into eight cornered brick elements. A brick element can be divided into five tetrahedra in two (and only two) distinct ways. This is shown in Fig. 2.2.

By averaging the displacement of the two types of subdivision, a slight improvement of accuracy can be obtained. Such elements could be assembled automatically from several tetrahedra and the process of creating these

tetrahedra left to a, logically, simple program. Similarly, each tetrahedral having 6 nodes splitted into three tetrahedra. This is shown in Fig. 2.3.

2.4 VOLUME COORDINATE :-

Once again special coordinates are introduced, defined by Fig. 2.4. A set of coordinates L_1, L_2, L_3 and L_4 for tetrahedral 1,2,3 and 4 is defined by a linear relationship between these and the cartesian system.

$$X = L_1x_1 + L_2x_2 + L_3x_3 + L_4x_4$$

$$Y = L_1y_1 + L_2y_2 + L_3y_3 + L_4y_4$$

$$Z = L_1z_1 + L_2z_2 + L_3z_3 + L_4z_4$$

$$1 = L_1+L_2+L_3+L_4 \qquad \text{----------} \qquad (5)$$

The physical nature of the coordinates can be identified as the ratio of the volumes of tetrahedra base an internal point P and the total volume, e.g. shown in Fig. 2.4. Therefore,

$$L_1 = \frac{\text{Volume P 234}}{\text{Volume 1234}} \qquad \text{and so on}$$

Solving Eqn. 6 for X, Y and Z

$$L_1 = (a_1+b_1x + c_1y + d_1z)/6V$$

$$L_2 = (a_2+b_2x + c_2y + d_2z)/6V$$

$$L_3 = (a_3+b_3x + c_3y + d_3z)/6V$$

$$L_4 = (a_4+b_4x + c_4y + d_4z)/6V \qquad \text{-----------} \qquad (6)$$

where

$$V = \frac{1}{6} \det \begin{vmatrix} 1 & x_1 & y_1 & z_1 \\ 1 & x_2 & y_2 & z_2 \\ 1 & x_3 & y_3 & z_3 \\ 1 & x_4 & y_4 & z_4 \end{vmatrix} \quad \text{-------------- (7)}$$

and

$$a_1 = \begin{vmatrix} x_2 & y_2 & z_2 \\ x_3 & y_3 & z_3 \\ x_4 & y_4 & z_4 \end{vmatrix} , \quad b_1 = - \begin{vmatrix} 1 & y_2 & z_2 \\ 1 & y_3 & z_3 \\ 1 & y_4 & z_4 \end{vmatrix}$$

$$c_1 = \begin{vmatrix} x_2 & 1 & z_2 \\ x_3 & 1 & z_3 \\ x_4 & 1 & z_4 \end{vmatrix} , \quad d_1 = - \begin{vmatrix} x_2 & y_2 & 1 \\ x_3 & y_3 & 1 \\ x_4 & y_4 & 1 \end{vmatrix} \quad \text{-----(8)}$$

Other coefficients are obtained by cyclic interchange of subscripts in order 1,2,3,4.

2.5 SHAPE FUNCTION :-

As the volume coordinates vary linearly with the cartesian ones from unity at one node to zero at the opposite face, the shape functions for linear element, are simply

$$N_1 = L_1 , \; N_2 = L_2, \; N_3 = L_3, \; N_4 = L_4$$

or

$$N_i = (a_i + b_i x + c_i y + d_i z)/6V \quad \text{---------(9)}$$

and

$$\{\delta\} = \begin{Bmatrix} U \\ V \\ W \end{Bmatrix} = [N] \; \{\delta\}^{(e)} \quad \text{--------- (10)}$$

where $\{\delta\}^{(e)}$ is defined by the twelve displacement components of the nodes. We can write the displacements of an arbitrary point within an element as

$$= [\ IN_1,\ IN_2,\ IN_3,\ IN_4] \{\delta\}^{(e)}$$

where, [I] being a 3x3 identify matrix. Once again the displacement functions used will obviously satisfy continuity requirements on interfaces between various elements. This fact is a direct corollary of the linear nature of the variation of displacements.

2.6 STRAIN MATRIX :-

The strain matrix can now be defined as

$$\{\epsilon\} = \begin{Bmatrix} \epsilon_x \\ \epsilon_y \\ \epsilon_z \\ \gamma_{xy} \\ \gamma_{yz} \\ \gamma_{xz} \end{Bmatrix} = \begin{Bmatrix} \frac{\partial u}{\partial x} \\ \frac{\partial v}{\partial y} \\ \frac{\partial w}{\partial z} \\ \frac{\partial u}{\partial y} + \frac{\partial v}{\partial x} \\ \frac{\partial v}{\partial z} + \frac{\partial w}{\partial y} \\ \frac{\partial w}{\partial x} + \frac{\partial v}{\partial z} \end{Bmatrix} \quad \text{---------} \quad (11)$$

Now

$$\{\epsilon\} = [B]\{\delta\}^{(e)} = [B_1,\ B_2,\ B_3,\ B_4]\{\delta\}^{(e)} \quad \text{---} (12)$$

In which,

$$[B_1] = \begin{bmatrix} \frac{\partial N_1}{\partial x} & 0 & 0 \\ 0 & \frac{\partial N_1}{\partial y} & 0 \\ 0 & 0 & \frac{\partial N_1}{\partial z} \\ \frac{\partial N_1}{\partial y} & \frac{\partial N_1}{\partial x} & 0 \\ 0 & \frac{\partial N_1}{\partial z} & \frac{\partial N_1}{\partial y} \\ \frac{\partial N_1}{\partial z} & 0 & \frac{\partial N_1}{\partial x} \end{bmatrix} = \frac{1}{6V} \begin{bmatrix} b_1 & 0 & 0 \\ 0 & c_1 & 0 \\ 0 & 0 & d_1 \\ c_1 & b_1 & 0 \\ 0 & d_1 & c_1 \\ d_1 & 0 & b_1 \end{bmatrix} \qquad \text{--------(13)}$$

where, submatrices of $[B_i]$ are obtained by cyclic interchange of subscripts 1,2,3,4.

2.7 ELASTIC STIFFNESS MATRIX :-

The first step in the application of the matrix displacement method is the determination of the stiffness characteristics of elements into which the structure is idealized. The elastic stiffness matrix for an element is desired by the application of principle of virtual displacements in a suitable form.

The strains, (ϵ) in an element are given by

$$(\epsilon) = [B]\{\delta\} \qquad \text{--------(14)}$$

where, $\{\delta\}$ is the vector of coefficients representing generalized displacements. The stresses in the element are given by

$$\{\sigma\} = [D]\{\epsilon\} \qquad \text{--------(15)}$$

where, $[D]$ is the elasticity matrix. The strain energy, U in the element becomes

$$U = \frac{1}{2} \int_{Vol.} \{\epsilon\}^T \{\sigma\} \, dV \qquad \text{--------- (16)}$$

From Eqns. 14 and 15, we can write the strain energy as

$$U = \frac{1}{2} \{\delta\}^T \left\{ \int_{vol.} [B]^T [D] [B] \, dV \right\} \{\delta\} \qquad \text{---------(17)}$$

Differentiating U with respect to $\{\delta\}$ twice we get the stiffness matrix $[K]^{(e)}$ with respect to the generalized coordinates $\{\delta\}$ as

$$[K]^{(e)} = \int_{vol.} [B]^T [D] [B] \, dV \qquad \text{---------(18)}$$

Let $[K]$ be the stiffness matrix with respect to the element nodal displacement $\{\delta\}^{(e)}$ which are related to $\{\delta\}$ by

$$\{\delta\}^{(e)} = [T]\{\delta\}$$

or

$$\{\delta\} = [T]^{-1} \{\delta\}^{(e)} \qquad \text{--------(19)}$$

where $[T]$ is a transformation matrix which is a square matrix.

The strain energy U in the element U with respect to the generalized coordinates $\{\delta\}$ is given by Eqn. 17

$$U = \frac{1}{2} \{\delta\}^T [K]^{(e)} \{\delta\}$$

From Eqn. 6, U becomes

$$U = \frac{1}{2} \{\delta\}^T [T^{-1}]^T [K]^{(e)} [T^{-1}] \{\delta\} \qquad \text{------- (20)}$$

The strain energy $U^{(e)}$ in the element with respect to the element nodal displacements is given by

$$U^{(e)} = \frac{1}{2} \{\delta\}^{(e)T} [K] \{\delta\}^{(e)} \quad \text{--------(21)}$$

Since the strain energy is independent of the coordinate system, we have

$$U = U^{(e)} \quad \text{-------------(22)}$$

Thus, from Eqns. 20-22, we obtain the element stiffness matrix $[K]^{(e)}$ with respect to the nodal displacements as,

$$[K] = [T^{-1}]^T [K]^{(e)} [T^{-1}] \quad \text{----------(23)}$$

Let $\{\rho\}$ be the vector of global displacements and is related to the nodal displacements $\{\delta\}^{(e)}$ by

$$\{\delta\} = [T] \{\delta\} \quad \text{------------(24)}$$

where, $[T]$ is a transformation matrix. The procedure given above for coordinate transformation Eqn. 23, also provide direct means of assembling the structure stiffness matrix $[K]$ from the element matrices $[K]^{(e)}$, both with respect to the nodal displacements.

Therefore,

$$[K] = [T]^T [K]^{(e)} [T] \quad \text{--------(25)}$$

2.8 MASS MATRIX :-

Assuming sinusoidal vibrations, the maximum kinetic energy, T of the element is given by

$$T = \frac{1}{2} \omega^2 \int_{vol.} [W]^T [W] \rho \, dV \quad \text{------(26)}$$

Let $[N]$ be the matrix of shape functions used to represent the displacement distribution $[W]$ over each element so that we can write T as

$$T = \frac{1}{2}\,\omega^2 \{\delta\}^T \left[\int_{vol.} \rho\, [N]^T [N]\, dV \right] \{\delta\} \qquad \text{-----(27)}$$

Differentiating T with respect to $\{\delta\}$ twice, we get the mass matrix $[m]^{(e)}$ with respect to the generalized coordinates $\{\delta\}$ as

$$[m]^{(e)} = \omega^2 \int_{vol} \rho\, [N]^T [N]\, dV \qquad \text{---------(28)}$$

where, ρ is the mass density.

We get the mass matrix $[m]^{(e)}$ with respect to the element nodal displacement $\{\delta\}$ as,

$$[m]^{(e)} = [T^{-1}]^T [m]^{(e)} [T^{-1}] \qquad \text{---------(29)}$$

and the assembled mass matrix $[M]$ as

$$[M] = [T]^T [m]^{(e)} [T] \qquad \text{--------(30)}$$

(see the Appendix for detail)

Finally, it leads to an eigen value problem as :

$$\{[K] - \lambda[M]\}\{\zeta\} = 0 \qquad \text{------(31)}$$

$$|[K] - \lambda[M]| = 0 \qquad \text{------(32)}$$

Solution part is being studied by a "simultaneous iteration algorithm for symmetric eigen value problems".

A simultaneous iteration is an extension of the power method. This algorithm is briefly summerized for determining sets of dominant eigen values and corresponding eigen vectors of symmetric matrices. The matrices are stored and processed in variable bandwidth forms; thus enabling advantage to be gained in economy on storage transfers when backing store needs to be used.

STEPS :-

Consider a matrix $[A]$ having eigen values λ_i such that $|\lambda_1| \geqslant |\lambda_2| \geqslant |\lambda_3| \ldots \geqslant |\lambda_n|$ and corresponding eigen vectors $q_1, q_2, q_3, \ldots\ldots, q_n$. If the eigen vectors are normalized so that the Euclidean norm of each is unity. then writing,

$$Q = [q_1, q_2, \ldots\ldots, q_n] \qquad \text{-------(33)}$$

the orthogonality condition for the eigen vectors gives

$$Q^T Q = I \qquad \text{---------(34)}$$

If $\{m\}$ trial vectors are to be processed simultaneously, these may be compounded into one matrix.

$$U = [U_1, U_2, \text{-------}, U_m] \qquad \text{--------(35)}$$

It will be assumed that they satisfy the orthogonality condition

$$U^T U = I \qquad \text{---------(36)}$$

The premultiplication operation

$$V = AU \qquad \text{-------(37)}$$

is the main step in the iterative process which makes the trial vectors converge into the domainant eigen vectors $q_1, q_2, q_3, \ldots\ldots\ldots\ldots, q_m$.

In Jennings' method the m x m symmetric interaction matrix

$$[B] = U^Y V = U^T A U \qquad \text{------------ (38)}$$

is determined. Then matrix T^* is constructed with unit diagonal elements and off-diagonal elements related to those of B according to

$$t^*_{ij} = \frac{-2b_{ij}}{(b_{ii}-b_{jj}) + s\sqrt{(b_{ii}-b_{jj})^2+16b^2_{ij}}} \qquad \text{---------- (39)}$$

where, s is the sign of $(b_{ii}-b_{jj})$.

The decoupled vector w then follow from the matrix multiplication

$$W = VT^* \qquad \text{--------(40)}$$

In this algorithm, V is initially copied into the store for W and then for each coefficient t^*_{ij} (j i), t_{ij}. V_j is added to W_i and t_{ij}. V_i is subtracted from W_j as soon as t^*_{ij} has been formed. In this manner, allocation of storage space for matrices B and T^* is avoided.

The diagonal elements b_{ii} give estimates of the eigen values which are used to save the trial vectors into their correct order according to dominance. Here variable bandwidth storage scheme [13] is used. The computer program developed in Ref.[13] is employed for obtaining the eigen values.

CHAPTER - 3

EXPERIMENTAL DETAILS

Experimental investigation has been carried out in order to find out the effects of flaws in laminated composite beams on natural frequencies. The various parameters considered are, stacking sequence, numbers and location of flaws and size of the specimen. The experimental investigation consists of the following stages.

1. Fabrication of laminated composite beams (with and without flaws) with different stacking sequences.
2. Characterisation of specimens.
3. Testing technique.

In what follows, each of these is separately discussed in detail.

3.1 FABRICATION :-

The present studies were carried out using epoxy resin as the matrix material and continuous glass fiber as the reinforcement. Epoxy resin (LY-556) and alphatic amines as its curing agent (HT-972),manufactured and marketed by ciba-geigy of India Ltd., under the trade names 'Araldite' and 'Hardner' respectively, were used. Continuous E-glass fibers, a product of Fiber-glass, Pilkington Ltd. of India, were used as the reinforcement material.

3.1.1 MECHANICAL PROPERTIES :-

1. Glass fiber : The mechanical properties of the fibers and matrix are

$E_f = 70 \ GN/m^2$

Density (ρ) = 25 $\frac{KN}{m^3}$

2. Epoxy : $E_m = 3.3 \ GN/m^2$ (determined experimentally

3.1.2 WINDING FRAME :-

In order to obtain good mechanical properties of the specimens, it is necessary to have uniform distribution of fibers throughout the matrix. For this purpose, a winding frame was designed and built. It consists of four mild steel strips of size (60cm x 5cm x 1cm) welded at the edges in such a way so as to get a frame of size (60cm x 60cm) .

Initial attempts to use a frame made of aluminium were unsuccessful. Due to inadequate stiffness, the configuration of aluminium frame changed during winding causing disorientation of fibers. No such problem is encountered with mild steel frames. Screws are fitted along the edges at a distance of 5mm from each other, in a zig-zag fashion for receiving the fibers. This results in a uniform distribution of fibers. Winding frame along with the fibers in tension employed for casting is shown in fig. 3.1.

3.1.3 MATRIX MATERIAL :-

Hand lay up technique was used. Therefore, the choice of the matrix material is restricted in the sense that it should have large curing time. This is achieved by suitably adjusting the hardner content. With this in view, the following matrix material and hardner, supplied by Ciba-Geigy of India Ltd. are used.

(a) Araldite LY-556

(b) Hardner HT-972

Table 3.1 shows the minimum curing time required at different curing temperatures. These curing times do not include the time required to bring the mould to the required temperature.

Araldite LY-556 and Hardner HT-972 in the ratio of 100:27 by weight is taken in a container (as specified by the company) and heated to a temperature of 80°-85°C. Fast stirring is done to ensure uniform temperature every where in the mixture. This process is carried out till the hardner is completely dissolved into the epoxy resin LY-556.

3.1.4 IMPREGNATION OF FIBERS :-

The above matrix solution will become more and more viscous as the temperature goes down. Once the solution becomes viscous it is very difficult to impregnate the fibers throughly. To avoid this problem the solution is poured on a single layer of fibers at a temperature 80°-85°C. To ensure

the complete impregnation of the fibers, rubber rollers under slight pressure are employed. After that, the specimen is left undisturbed for about 24 hours (depending upon the room temperature) so that it gets into the semi viscous state. The reason for this being that the fiber orientation should not change while cutting a single layer of fiber in a desired angle and size of the lamina.

The time required to attain the above mentioned semi-cured state is established through various trials. Table 3.2 shows the time required for matrix material to reach semi cured state at different room temperatures. The times shown in this table are approximate. However, a variation of one hour on either side does not effect the results substantially. But, if the variation is on the higher side, the material will get cured completely and the possibility of occurance of delamination increases. If the variation is on the lower side, the chances of disorientation of the fiber and overflow of resin is a possibility. Plates in a semi viscous state are then removed from the frame. With the help of a diamond cutter it is cut into desired sizes and orientations. Plies in a desired order of orientation are placed one above the other. The entire stack with a mylor sheet on the top and bottom surfaces is placed between two aluminium plates, which in turn is kept in a hot press.

3.1.5 CURING :-

These stacks have to be cured so that the polymerization is complete. This results in a laminated sheet of the desired strength. The required curing temperature (120°C) and pressure (50kg/cm^2) is applied. During the process of curing following problems arise and these have to be taken care of.

(a) Bulging of material : At high temperatures, the epoxy regains the viscous form and hence under pressure it starts flowing causing disorientation in fibers which in turn change the mechanical properties of the material. To overcome this problem a die is used which has been designed and fabricated.

(b) Sticking of the surfaces : Epoxy sticks to the mylor sheet. It can be taken care of, by the use of releasing agents like waxpol or mould releasing agents.

3.1.6 DIE :-

It consists of a mild steel plate of size (38cm x 20cmx2.5cm with a capability of receiving a sheet of the size (30cm x 10cmx 2.5cm) in it and is fixed on a plate size (38cmx20cmx1.25cm) with counter sunk screws as shown in fig. 3.2a. Another plate of the same size is also fixed on a plate of size (38cm x 20cm x 1.25cm) as shown in fig. 3.2b. This complete set acts as a die. All the surfaces of die, which come in contact with the specimen are polished so as to get smooth surfaces.

Curing temperature of 120°C and pressure of 50kg/cm^2 are maintained for about one hour. This ensures the complete curing of the specimen.

Flaw of a desired size and shape was created during the process of curing by introducing a thin strip of metallic material in the laminated specimen at a desired location. After the curing is complete the metal strip is removed which results in a flaw. Finishing of the shape is done by using the tools. For experimental investigations, specimens with following stacking sequences have been fabricated. The method of fabrication adopted is quite versatile and can be used to fabricate laminated plates of any desired fiber orientation.

1. Only matrix
2. All fibers in longitudinal direction
2. All fibers in transverse direction
4. All fibers aligned at 45°
5. Layers with stacking sequence (0/90/0/90/0)
6. Layers with stacking sequence (0/45/90/45/0)
7. Layers with stacking sequence(30/-30/30/-30/30)
8. Layers with stacking sequence (45/-45/45/-45/45)
9. Layers with stacking sequence (60/-60/60/-60/60)

Specimens from 1-4 are used for characterising the specimen and to obtain the elastic constants E_m, E_L, E_T and G_{LT} and the effect of flaws are studied using the laminated samples.

Following precautions are suggested to be observed throughout the fabrication process for obtaining specimens which have good mechanical properties.

1. The fibers should not be stresed unevenly. Otherwise, the fibers will not be aligned in the desired direction. Further, it is possible that some fibers may break during the rolling process. Only sufficient tension is to be applied (which is a matter of experience) to maintain the desired fiber orientation.

2. The thickness of the specimen is a critical parameter. It has to be uniform throughout the length of the specimen. Because of the flexible dies, variation in thickness along the length of the specimen is quite possible. Die should be kept in the press carefully so that there is no gap between the die and spacers.

3. If the extra epoxy from the impregnated fibers is not squeezed out, the percentage of fiber volume fraction reduces, resulting in a reduction of strength, which in turn effects the natural frequency of the specimen. Here, proper care should be taken during squeezing of the epoxy from impregnated fibers. For this, rubber rollers have to be rolled over it with a slight pressure.

4. The percentage of hardener in epoxy is very important. Inadequate amount of hardener results in a poor strength. On the other hand, excessive amount of hardner causes the epoxy to set quickly.

5. Pressure and temperature should be maintained at constant values, within the range of 5-10 percent.

3.2 CHARACTERISATION :-

3.2.1 BURN TEST :-

This test is carried out to determine the percentage volume fraction of fibers in the composite which in turn indicates the strength of composite. A piece of specimen is cut and weighed in a crucible by an electronic balance. The weight of the empty crucible is taken. The crucible along with the specimen is placed in a furnace at 700°c. for about 7 hours, and removed when the matrix is completely burnt, leaving only the glass fibers. The weight of crucible and burnt specimen is taken. Using this data the percentage volume fraction of fibers is determined for one specimen which is given in table 3.3.

3.2.2 Determination of Elastic Constants :-

To determine the elastic constants in longitudinal, transverse and 45°, the specimens of size (14cm x 2.3cm x 0.29cm) have been taken and tested on a material testing machine . The plot between load and displacement for various specimen gives the values of E_L, E_T and E_X for fiber volume fraction of 0.27.

For obtaining poisson's ratio, ν_{LT}, two strain ganges are used, one along the length of the fiber and other transverse to it , They are fixed on a specimen having all the fibers

aligned at 0°. The longitudinal strain, ϵ_L, and transverse strain ϵ_T for the same load are given in table 3.4. The Poisson's ratio LT may be determined from the above data by using the formula

$$\nu_{LT} = -\frac{\epsilon_L}{\epsilon_T}$$

3.3 TEST SET UP :-

The experimental setup is shown in fig. 3.3. Frequency spectrum is scanned gradually for the range 15c/s - 350 c/s for the reason that the theoritical value of the first natural frequencies, for the type of specimen investigated are much above 15 c/s and the value of second natural frequency are much below 350c/s slow scanning is done starting from 15 c/s and the corresponding amplitude is observed on the oscilloscope screen. The frequency corresponding to various modes are identified by the Lissajous figures on the oscilloscope. Before performing the experiments care should be taken that continuity of strain gauge is checked with the help of strain gauge indicator and to ensure that the bridge circuit is in balanced position.

A frequency corresponding to the maximum amplitude for a given input is taken as a measure of the natural frequency.

Specimen with various stacking sequence and with flaw and without flaws and different lengths are tested with boundary conditions being simply-supported and clamped-clamped and the results are presented in the next chapter.

CHAPTER - IV

RESULTS AND DISCUSSION

4.1 MATERIAL CHARACTERIZATION :-

The laminated composite beams with and without flaws at various locations are tested for two different boundary conditions namely simply supported and clamped-clamped. The beams are tested for different stacking sequence and various flaw locations. The theoretical and experimental results are presented in the form of graphs and tables.

Fig. 4.1 shows the experimental plot of stress versus strain for a specimen with fiber volume fraction of 27 percent, obtained directly from the material testing machine. The value of elastic modulus in longitudinal direction, E_L, calculated from this plot is 30.61×10^4 kg/cm^2 (29 GN/m^2).

Fig. 4.2 shows the experimental plot of stress versus strain for a similar specimen with all the fibers in transverse direction. The transverse modulus, E_T, is found to be 8.23×10^4 kg/cm^2 (8.2 GN/m^2).

From Fig. 4.3, the value of poisson's ratio ν_{LT} is obtained and is found to be 0.346.

The value of poisson's ratio ν_{TL} as obtained from the set of experiments shown in fig. 4.4 is 0.09224. This is also checked and corroborated from the relation $E_L/E_T = \nu_{LT}/\nu_{TL}$.

Fig. 4.5 shows the plot of stress versus strain for specimen having all the fibers aligned at 45° to the loading axis. The value of E_x obtained from this plot is 7.97×10^4 kg/cm^2 (7.9 GN/m^2).

The value of shear modulus, G_{LT} obtained from the experimental values of E_L, E_T, E_x and ν_{LT} (see appendix) is 2.7×10^4 kg/cm^2 (2.7 GN/m^2).

$$\nu_{TL} = -\frac{\epsilon_L}{\epsilon_T}$$

From fig. 4.4, the value of strain in the longitudinal direction, ϵ_L is found to be -12.0 and strain in the transverse direction, ϵ_T is found to be 130.0.

Therefore,

$$\nu_{TL} = -\left(\frac{-12.0}{130.0}\right)$$

$$= 0.09224 \text{ (experimentally determined)}$$

Also,

$$\frac{\nu_{LT}}{E_L} = \frac{\nu_{TL}}{E_T}$$

$$\nu_{TL} = \frac{E_T}{E_L} \cdot \nu_{LT}$$

by substituting the values of E_L, E_T & ν_{LT} we again get ν_{TL} as shown below.

$$\nu_{TL} = 0.346 \times \frac{82345.6}{306122.4}$$

$$= 0.093 \text{ (computed)}$$

4.2 BEAM VIBRATION :-

Laminated composite simply-supported and clamped-clamped beams (with and without flaws), with different stacking sequences [30/-30/30/-30/30] , [45/-45/45/-45/45], [60/-60/60/-60/6 [0/45/90/45/0] , [0/90/0/90/0] are tested for natural frequencies using single point excitation at the mid span for the beam.

Table 4.2.1 gives the results of natural frequencies for different fiber orientations and stacking sequences. This table also indicates the frequency obtained for different flaw dimensions. Theoretical results obtained using finite element analysis as discussed in Chapter 2, are also given in the same table. The experimental values are based on the average value obtained from a test of 4 samples each. It is observed that experimental results are almost in close agreement with theoretical values. Further, as the flaw size increases the frequency decreases for all the three stacking sequences.

Fig. 4.2.1 shows the plot of the first natural frequency versus the fiber orientation obtained experimentally for a simply-supported laminated beam. Theoretical results are also plotted. It is observed that as the fiber orientation increases, the frequency decreases. The behaviour can be explained as indicated below.

$$\bar{Q}_{11} = Q_{11} \cos^4\theta + 2(Q_{12} + 2Q_{66}) \sin^2\theta \cos^2\theta + Q_{22} \sin^4\theta \qquad \text{------(4.2.1)}$$

The values are computed for $\theta=30°$ and $\theta=45°$ by knowing Q_{11}, Q_{12}, Q_{66} and Q_{22}.

$(\bar{Q}_{11})_{30°} = 243182.01$ kg/cm^2

and

$(\bar{Q}_{11})_{45°} = 200246.15$ kg/cm^2

It is clear from the above values that $\bar{Q}_{11}$ is maximum for $\theta=30°$ and hence the D_{11} and at $\theta=45°$, $\bar{Q}_{11}$ is minimum and hence D_{11}.

It is observed from the graph that the 45° fiber orientation lies above the 60° fiber orientation point. It has been shown in Ref. [14] that this could be due to high interlaminar shear stresses and that the inter laminar normal stresses are very dependent on stacking sequence, which could develop due to -45° fiber orientation ply.

Table 4.2.2 and 4.2.3 gives the results of natural frequency with length of the specimen for [60/-60/60/-60/60] and [30/-30/30/-30/30] fiber orientation for a simply supported laminated beam. It is observed from the tables that the natural frequency decreses as the flaw size increases. Further, it is observed that reduction in frequencies for [60/-60/60/-60/60] fiber orientation laminate is less than [30/-30/30/-30/30] fiber orientation laminate.

Fig. 4.2.2 and Fig. 4.2.3 shows the response of a simply supported beam with varying length for two stacking

sequences. From the curve it is observed that although there is a reduction in frequency as the flaw size increases the curve tends to be flat with increase in length of specimen. Further, the effect of flaw also reduces with increase in length.

Fig. 4.2.4 shows the variation of frequency with flaw area. It is observed that reduction in frequency for 30° fiber orientation is much more than at 60° fiber orientation. It could be due to the fact that the stiffness of the beam at 30° is much higher as compared to the one of 60° fiber orientation. Further more, it is observed that the frequency is not very much effected with area of flaw for 60° fiber orientation. The frequency decreases after a critical value of the flaw area.

Table 4.2.4 shows the results of natural frequency variation with fiber orientation for clamped-clamped flaw less beam. This table also indicates the frequency obtained for different flaw, area.

Fig. 4.2.5 shows the natural frequency variation with fiber orientation for clamped-clamped flaw less beam. The observations made with regard to the simply-supported beam are valid here also.

Table 4.2.5 gives the variation of natural frequency with length of the specimen for clamped-clamped for [30/-30/30/-30/30] fiber orientation laminate.

Fig. 4.2.6 and Fig. 4.2.7 shows a typical plot of the response for a fiber orientation of 30° for a clamped-clamped beam for different flaw areas. This plot shows that as the length decreases frequency correspondingly increases. Further it is observed that the effect of flaw is felt more when beam length is smaller. This could be due to the reduction in the bending energy for a given flaw is more for shorter beam as compared to longer beam.

Table 4-2.6 gives the results of natural frequency variation with length of the specimen for [0/45/90/45/0] fiber orientation for clamped-clamped beam.

Fig. 4.2.8 shows (A typical plot of fiber orientation of [0/45/90/45/0]) that as the length increases the natural frequency decreases. Further, it is observed that reduction in natural frequency for 30° fiber orientation is much more as compared to [0/45/90/45/0] laminate.

Table 4.2.7 gives the variation of natural frequency with length of specimen for clamped-clamped beam for [0/90/0/90/0] fiber orientation.

Fig. 4.2.9 shows (A typical example of cross ply laminate) that as the length decreases, the natural frequency increases. Further, it is observed that as the flaw area increases there is a reduction in the natural frequency. It is also observed that [0/45/90/45/0] laminate is stiffer than [0/90/0/90/0] laminate.

Fig. 4.2.10 shows (A typical example of comparision between cross ply laminate and [0/45/90/45/0] laminate) that as the flaw area increases there is a decrement in natural frequency monotonically. This could be due to delamination.

Table 4.2.8 gives the variation of natural frequency with length of specimen for clamped-clamped beam for [60/-60/60/-60/60] fiber orientation.

Fig. 4.2.11 shows (A typical example of [60/-60/60/-60/60] fiber orientation laminate) variation of natural frequency with length of the specimen. Further it is observed that [60/-60/60/-60/60] laminate is much more stiffer than the [30/-30/30/-30/30] laminate, as shown in Fig. 4.2.6.

Fig. 4.2.12 shows the plot of two different stacking sequences for various flaw area with natural frequencies for a clamped-clamped beam. The observation made with regards to simply-supported beam is valid here also.

CHAPTER - V

CONCLUSIONS

1. For the beam studied it is observed that the first natural frequency decreases monotonically when fiber orientation increases from 0° to 90° flaws are more effective for small orientations.

2. Reduction in first natural frequency increases with increase in flaw area.

3. The natural frequency decreases with increase in length of the specimens, also the effect of flaw in reducing natural frequency is more for smaller lengths.

4. Effect of flaw on the natural frequency increases is the flaw location moves from structure reference axis towards Top or bottom surface of the specimen.

5. Decrement in first natural frequency is maximum when flaw is exactly at middle for simply supported beam.

6. For clamped-clamped condition the reduction in frequency is more as compared to simply supported.

TABLE - 3.1.1

Variation of curing time with temperature

Curing °C	Temperature °F	Minimum curing time
80	176	10-12 hrs
100	212	3 - 4 hrs
140	284	1 - 2 hrs
180	356	10 - 30 hrs

TABLE - 3.1.2

Variation of time required for material to reach semicured state with room temperature

Room temperature °C	Time
15 - 18	30 hrs
22 - 26	24 hrs
30 - 36	18 hrs

TABLE - 3.1.3

Percentage volume fraction of fibers

Empty weight of crucible	=	9.66 gms.
weight of specimen	=	14.38 gms.
weight of crucible + specimen	=	24.04 gms.
Total weight after matrix burnt	=	15.99 gms.
fiber weight or residue weight	=	6.33 gms
weight fraction	=	$\frac{6.33 \text{ gms}}{14.38 \text{ gms}} = .44 = 44\%$
specific gravity of epoxy	=	1.18
specific gravity of fiber	=	2.54

$$\rho_c = \frac{1}{\sum \frac{w_i}{\rho_i}}$$

$$= \frac{1}{\frac{0.44}{2.54} + \frac{0.56}{1.18}} = 1.544 \quad gm/cm^3$$

$$\text{Percentage volume fraction of fiber} = \frac{\rho_c \times \text{wt. fraction}}{\text{specific gravity of fiber}}$$

$$= \frac{1.544 \times 0.44}{2.54}$$

$$V_f = 26.73\%$$

TABLE - 4.2.1

Variation of first natural frequency with fiber orientation for a specimen of length L=27.0 cm (Simply-supported)

Orientation	flaw less natural frequency (c/s)	Natural frequency with flaw of (c/s)		
		1cm on one side of reference axis	2 cm. on one side of reference axis	3 cm. on one side of reference ax
[30/-30/30/-30/30]	(61.3)*	(60.6)	(60.2)	(59.8)
	63.0	62.2	61.8	60.7
[45/-45/45/-45/45]	(60.0)	(59.3)	(58.8)	(58.4)
	60.71	60.1	59.6	59.05
[60/-60/60/-60/60]	(57.1)	(57.1)	(56.9)	(56.05)
	60.0	59.8	59.7	59.6

* The quantities inside the parenthesis indicate the experimental values

TABLE - 4.2.2

Variation of natural frequency with length of the specimen [60/-60/60/-60/60] laminate (simply supported)

Length (cm)	Flaw less natural frequencies (c/s)				Ist natural frequency with flaw of (c/s)				
	Ist	3rd	5th	7th	1cm on one side of ref. axis	2cm on one side of ref. axis	1cm on both side of ref.axis	2cm on both side of ref. axis	3cm on both side o ref. a
27.4	(57.0) 59.59	(162.7)	(239.1)	(659.8)	(57.[illegible])* 59.55	(56.9) 59.45	(56.8) 59.23	(56.6) 59.31	(56.2) 59.19
27.0	(57.1) 60.0	(162.7)	(239.1)	(695.8)	(57.1) 59.9	(57.0) 59.8	(56.8) 59.7	(56.7) 59.6	(56.2) 59.3
26.0	(59.9) 62.92	(163.8)	(240.8)	(700.3)	(59.8) 62.53	(59.0) 62.01	(58.5) 61.72	(57.0) 61.51	(56.5) 60.70

* The quantities inside the Parenthesis indicate the experimental values.

TABLE - 4.2.3

Variation of natural frequency with length of the specimen [30/-30/30/-30/30] laminate

Length	Flaw less natural frequencies (c/s)				Ist natural frequency with flaw of (c/m)		
	Ist	3rd	5th	7th	1cm on one side of ref. axis	2cm on one side of ref. axis	3 cm on one side of ref. axis
27.4	(60.5)*	(166.7)	(583.5)	(708.35)	(60.2)	(59.9)	(59.0)
	62.0				61.37	61.3	59.96
27.0	(61.3)	(168.68)	(609.75)	(740.8)	(61.1)	(60.2)	(59.85)
	63.0				62.2	61.8	60.75
26.0	(64.0)	(180.6)	(614.4)	(815.05)	(63.9)	(63.6)	(61.3)
	65.0				64.899	63.99	62.8

* The quantities inside the parenthesis indicate the experimental values.

TABLE - 4.2.4

Variation of first natural frequency with fiber orientation and for different flaw dimensions for a spec. of length L=26.0cm (clamped-clamped)

Orientation	Flaw less natural frequency (c/s)	First Natural frequency with flaw of (c/s)		
		1 cm on one side of reference axis	2cm on one side of reference axis	3 cm on one side of ref. axis
[30/-30/30/-30/30]	(93.2)*	(91.9)	(89.7)	(89.0)
	95.0	94.21	92.60	91.01
[45/-45/45/-45/45]	(87.6)	(86.4)	(35.2)	(84.3)
	90.40	88.24	87.31	86.24
[60/-60/60/-60/60]	(84.0)	(83.3)	(82.0)	(81.7)
	85.90	85.60	84.52	84.32

* The quantities inside the parenthesis indicate the experimental values.

TABLE - 4.2.5

Variation of natural frequency with length of specimen 30/-30/30/-30/30 laminate (clamped-clamped)

Length	Flaw less Ist natural frequency (c/s)	Ist natural frequency with flaw of (c/s)			
		1 cm on one side of ref. axis	2cm on one side of ref. axis	1cm on both side of ref. axis	2cm on both side of ref.axis
27.0	(87.5)*	(86.3)	(84.9)	(85.8)	(84.2)
	89.3	88.7	87.1	87.7	85.2
26.0	(93.2)	(91.9)	(89.7)	(90.9)	(88.6)
	95.0	94.2	92.6	93.4	90.4
25.0	(96.45)	(97.5)	(94.7)	(96.3)	(92.2)
	100.6	99.6	98.0	98.95	95.5

* The quantities inside the parenthesis indicate the experimental values.

TABLE - 4.2.6

Variation of natural frequency with length of specimen [0/45/90/45/0] laminate (clamped-clamped)

Length	Flaw less Ist natural frequency (c/s)	Ist natural frequency with flaw of (c/s)			
		1cm on one side of ref. axis	2cm on one side of ref. axis	1cm on both side of ref. axis	2cm on both side of ref. axis
27.4	(94.0)*	(94.0)	(92.6)	(93.5)	(91.5)
	95.102	93.8	93.6	93.8	93.0
27.0	(95.6)	(95.0)	(93.9)	(94.8)	(93.1)
	96.8	96.4	95.2	95.6	94.4
26.0	(100.1)	(99.4)	(97.5)	(97.6)	(96.4)
	101.12	100.5	99.2	99.8	98.0

* The quantities inside the parenthesis indicate the experimental values.

TABLE - 4.2.7

Variation of natural frequency with length of specimen [0/90/0/90/0] laminate
(clamped-clamped)

Length	Flaw less Ist natural frequency (c/s)	Ist natural frequency with flaw of (c/s)			
		1cm on one side of ref. axis	2cm on one side of ref. axis	1cm on both side of ref. axis	2cm on both side of ref. axis
27.4	(111.0)*	(110.0)	(108.6)	(108.1)	(106.6)
	112.42	116.02	110.12	110.41	107.01
27.0	(112.7)	(112.0)	(110.4)	(109.8)	(107.6)
	114.2	113.30	111.6	112.1	108.6
26.0	(117.05)	(116.0)	(114.6)	(112.0)	(111.2)
	118.5	117.6	115.8	116.3	112.6
25	(121.01)	(120.0)	(118.8)	(118.0)	115.4)
	122.8	121.94	119.5	120.4	116.8

TABLE - 4.2.8

Variation of natural frequency with length of specimen [60/-60/60/-60/60] laminate (clamped-clamped)

Length	Flaw less Ist natural frequency (c/s)	Ist natural of frequency with flaw of (c/s)			
		1cm on one side of ref. axis	2cm on one side of ref. axis	1cm on both side of ref. axis	2cm on both side of ref. axis
27.0	(79.8)*	(79.1)	(78.0)	(78.9)	(77.9)
	81.3	81.1	80.06	80.7	79.4
26.0	(84.0)	(83.3)	(82.0)	(82.6)	(81.8)
	85.89	85.6	84.5	85.1	83.7
25.0	(89.01)	(88.3)	(87.1)	(87.5)	(86.8)
	91.2	90.1	89.06	89.51	88.5
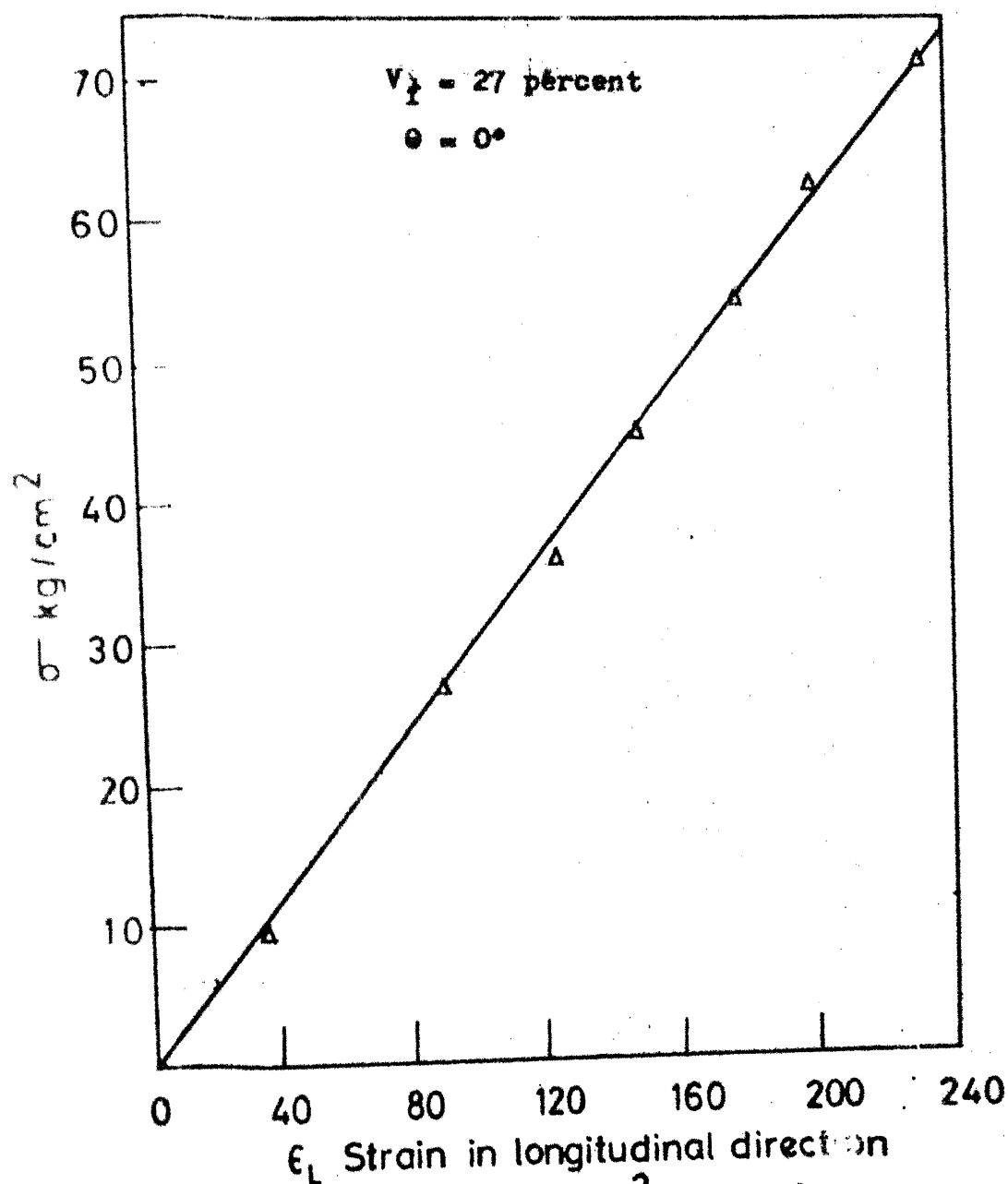
FIG.- 1 VARIATION OF σ kg/cm^2 WITH ϵ_L
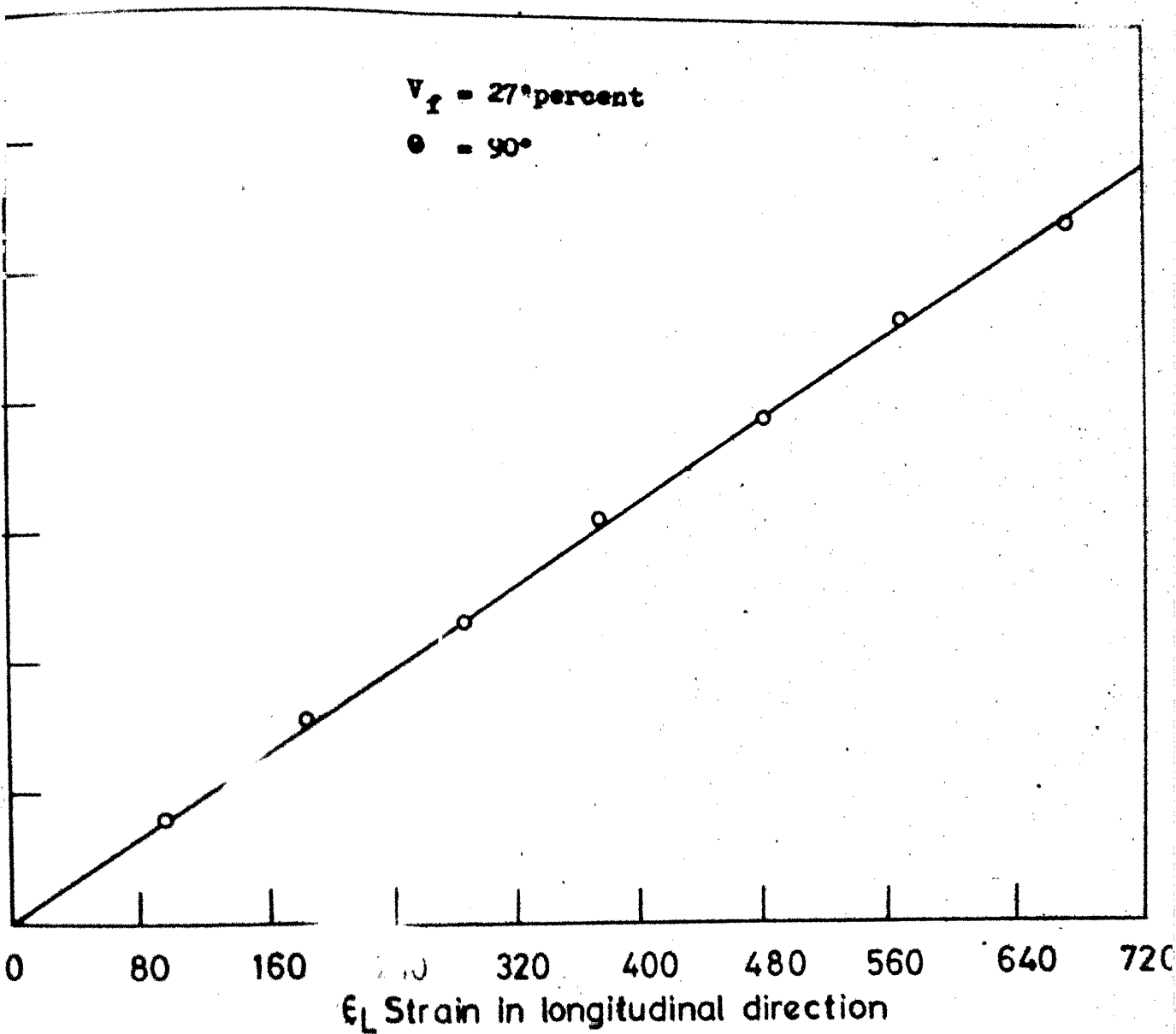
FIG. 4.2 VARIATION OF σ kg/cm² WITH ϵ_L
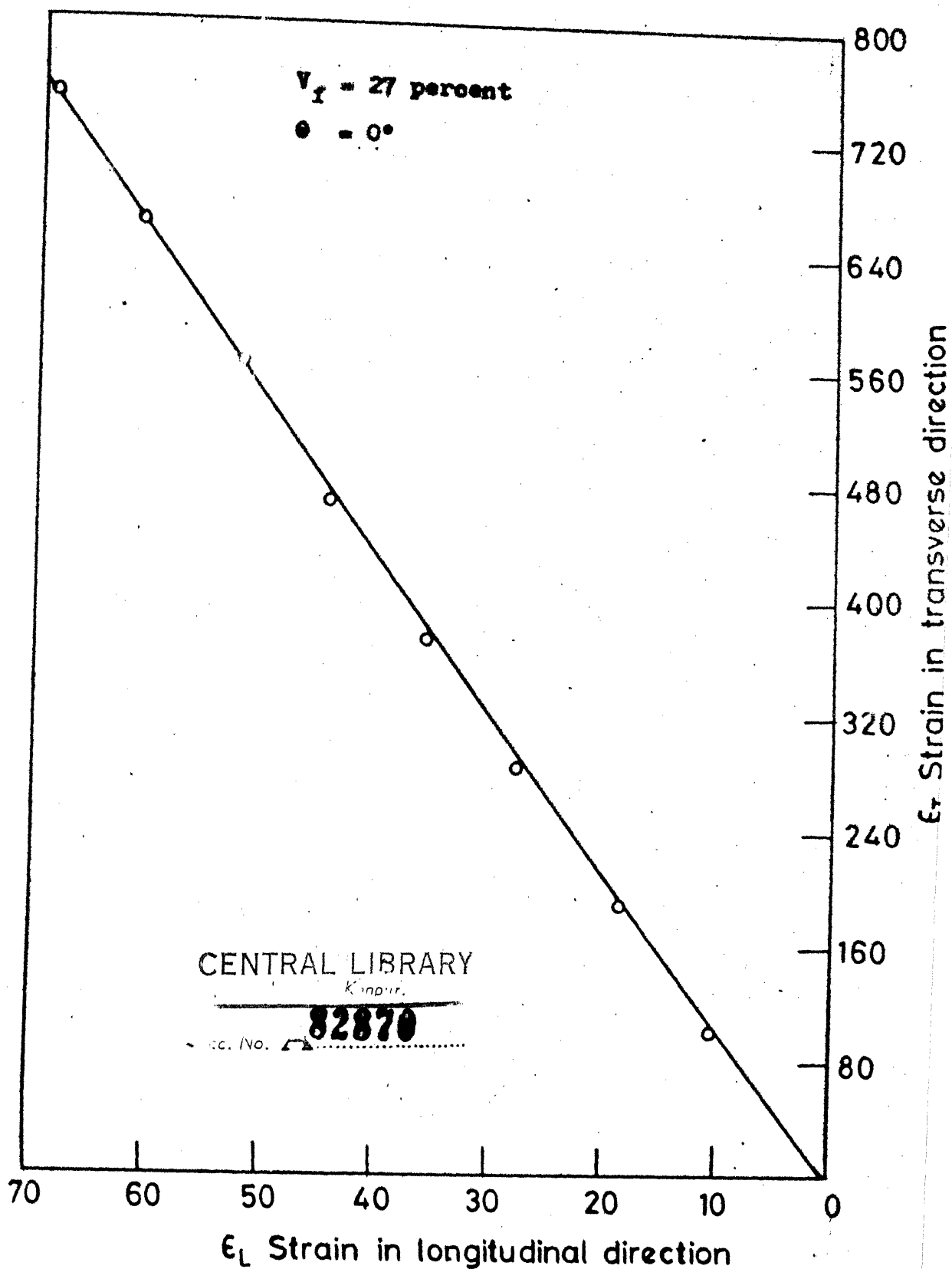
FIG. 4.3 VARIATION OF STRAIN IN TRANSVERSE WITH LONGITUDINAL DIRECTION
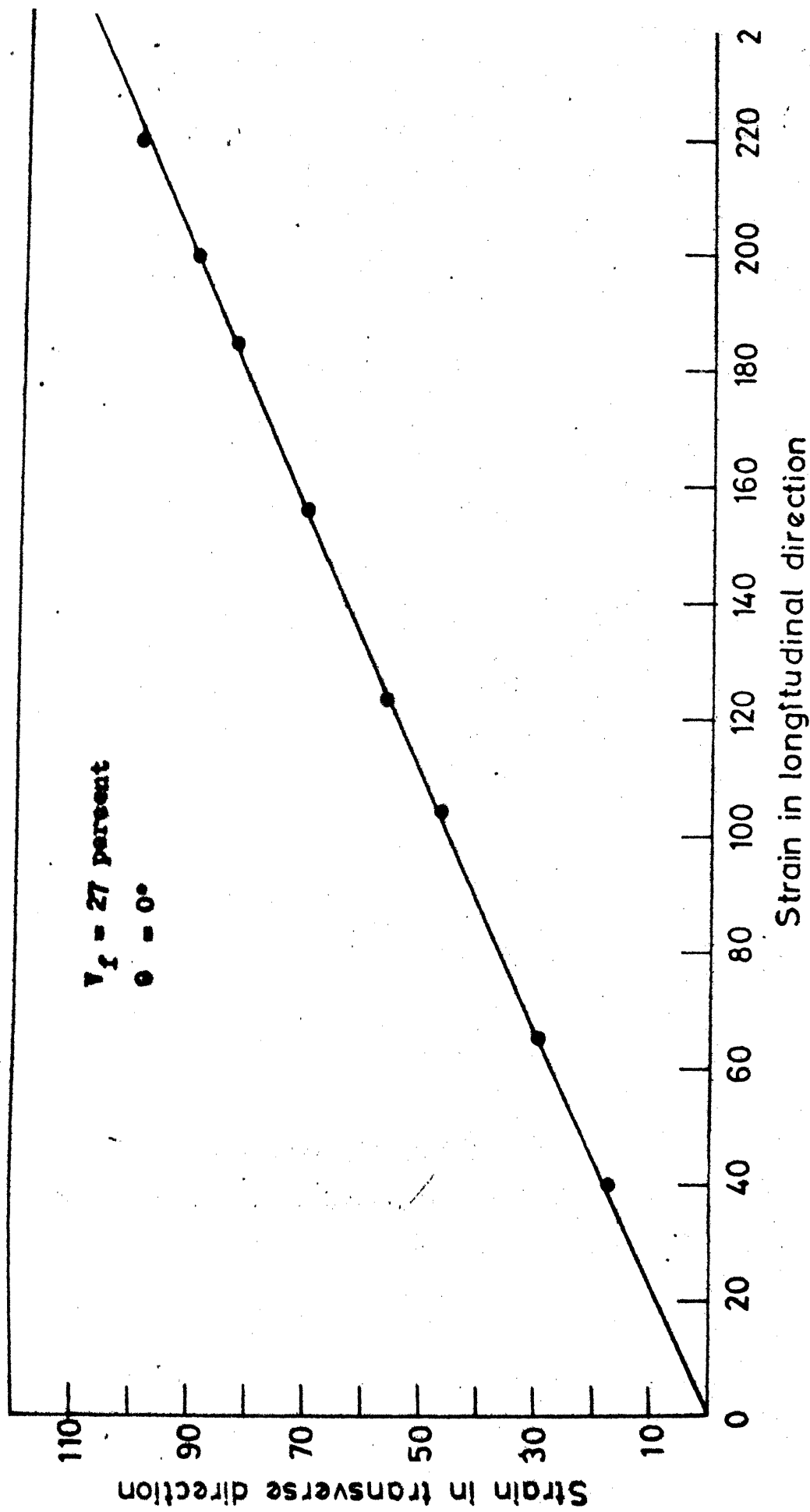
FIG. 4.4 VARIATION OF STRAIN IN TRANSVERSE WITH LONGITUDINAL DIRECTION
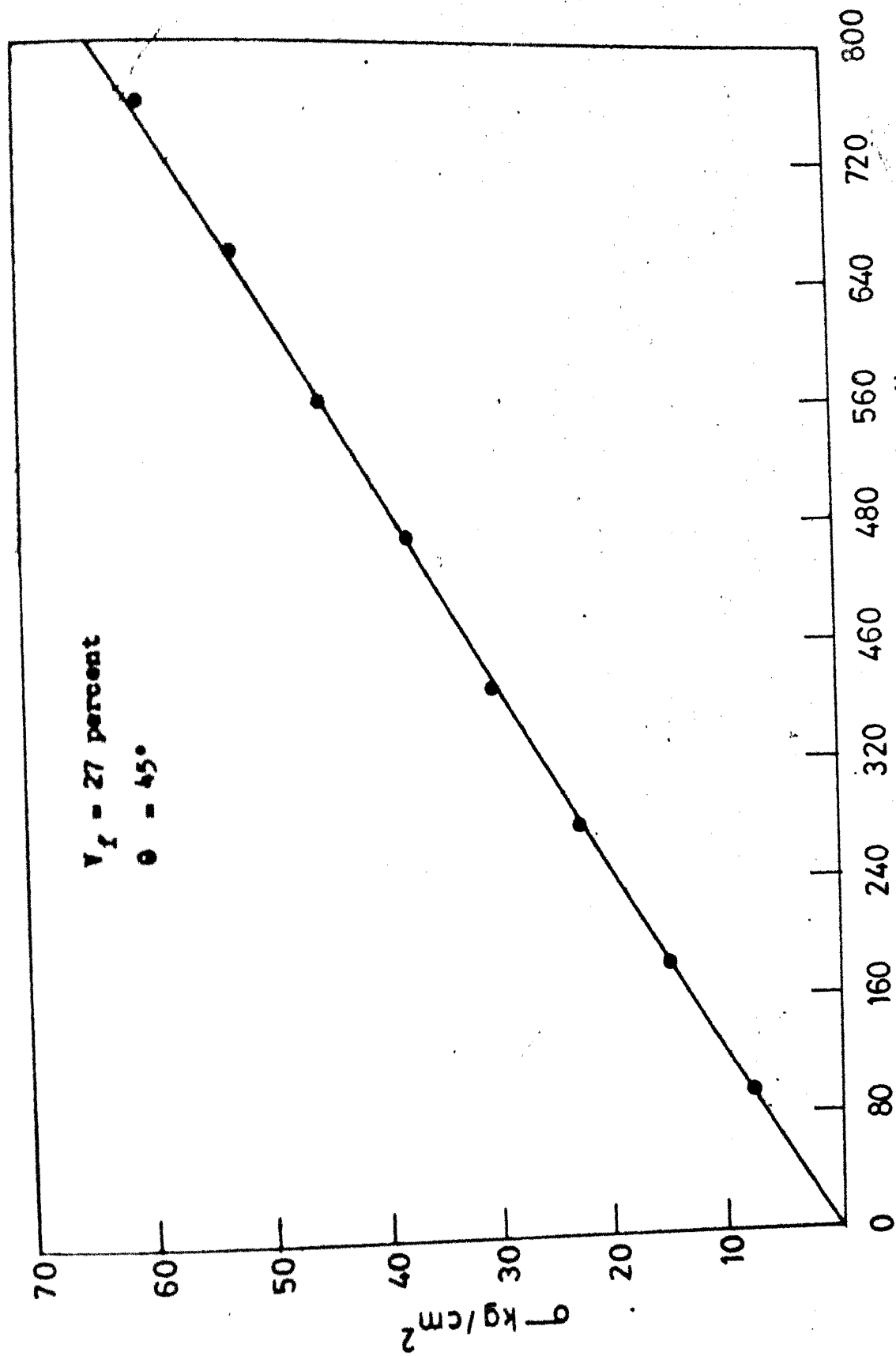
FIG. 4.5 VARIATION OF σ kg/cm^2 WITH LONGITUDINAL DIRECTION
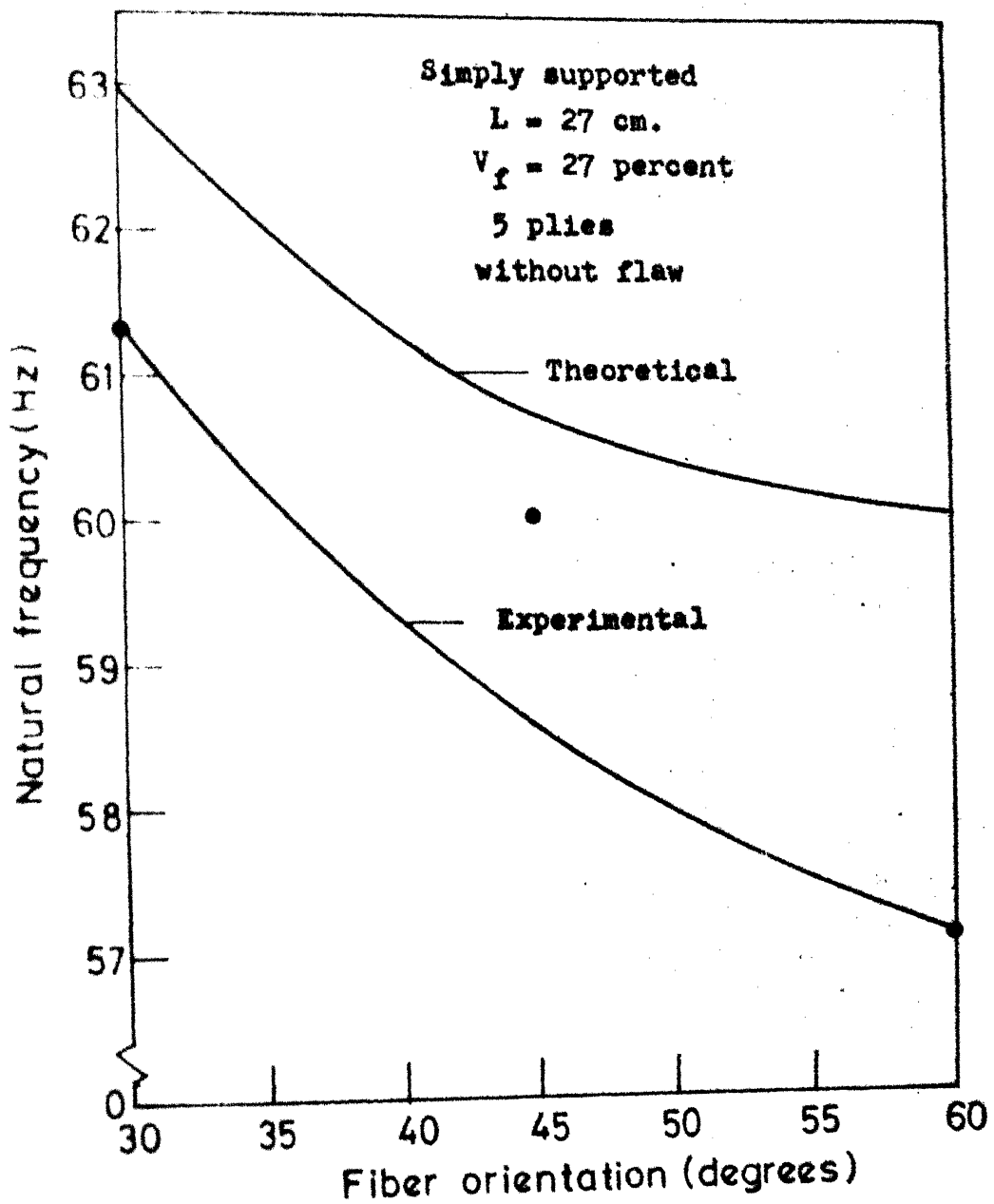
FIG. 4.2.1 VARIATION OF NATURAL FREQUENCY WITH FIBER ORIENTATION.
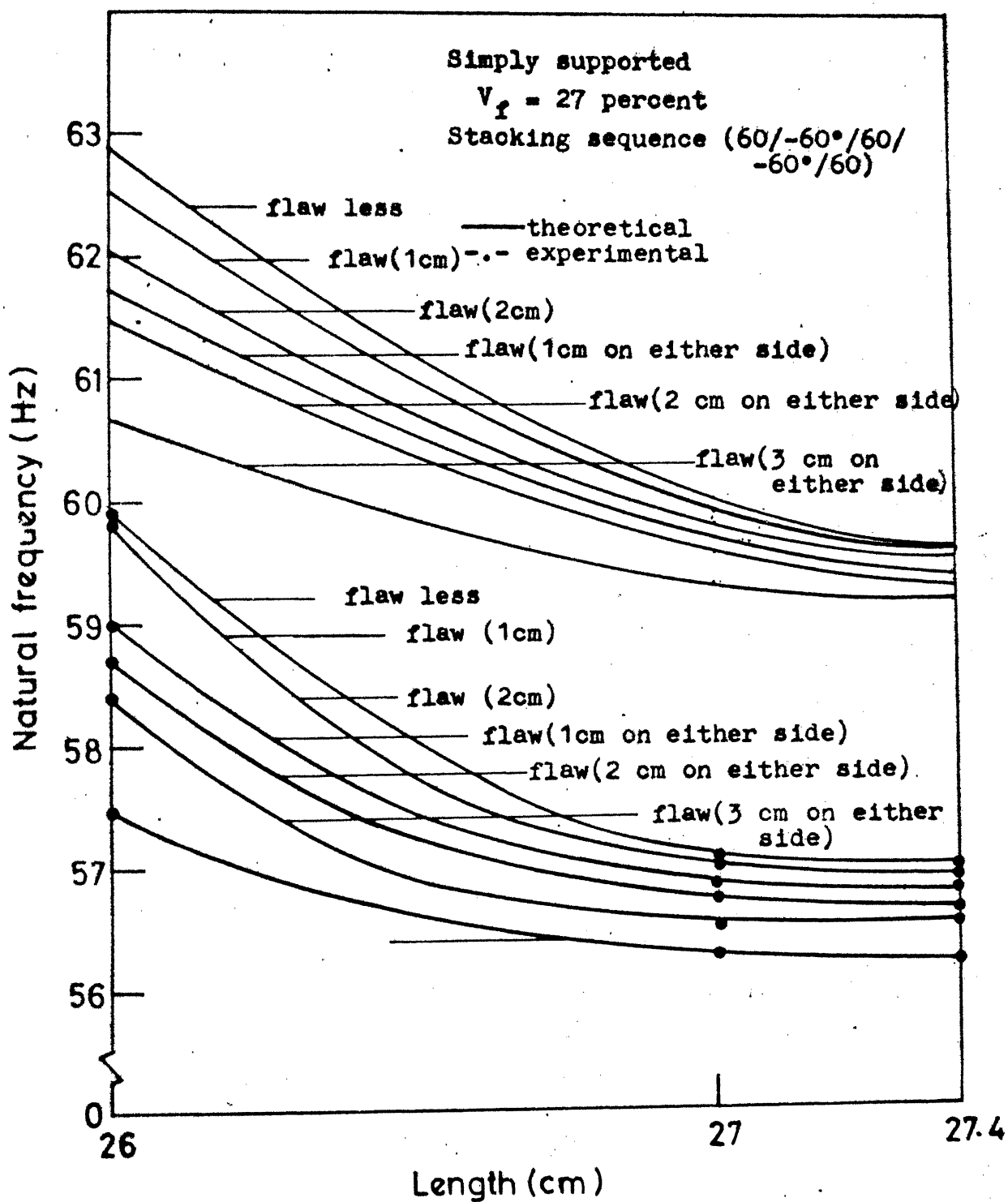
FIG. 4.2.2 VARIATION OF NATURAL FREQUENCY WITH LENGTH
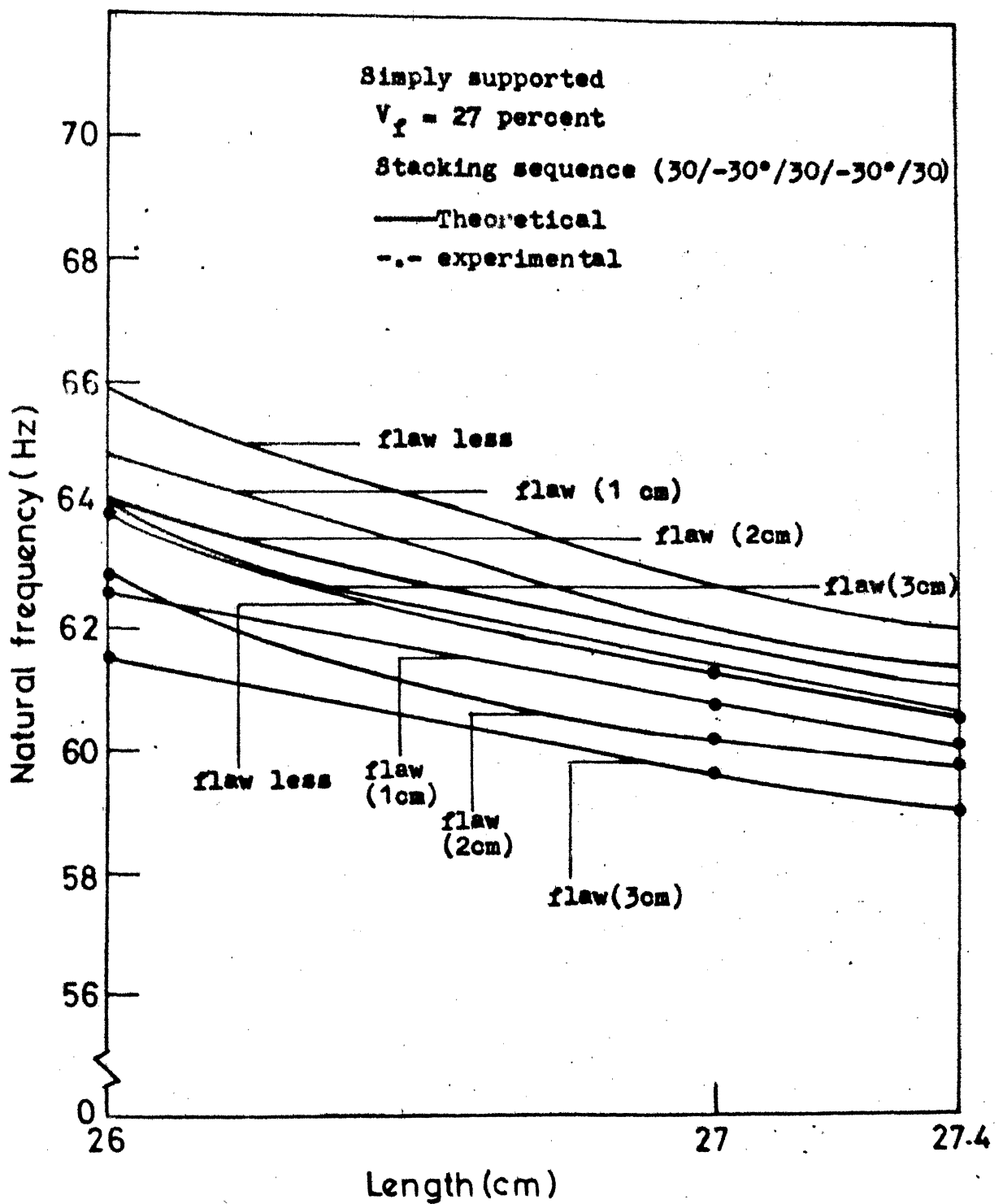
FIG 4.2.3 VARIATION OF NATURAL FREQUENCY WITH LENGTH
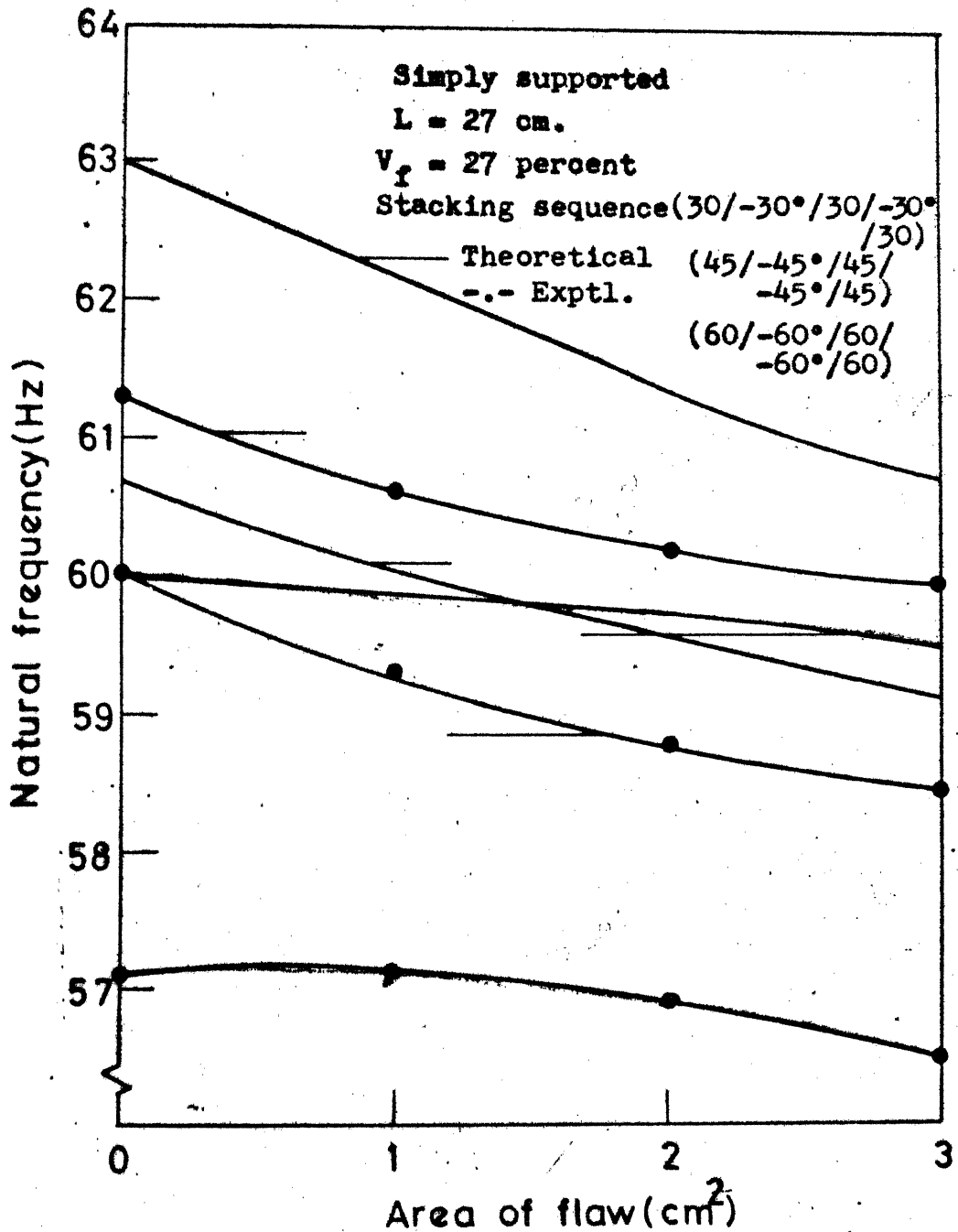
FIG. 4.2.4 VARIATION OF NATURAL FREQUENCY WITH AREA OF FLAW
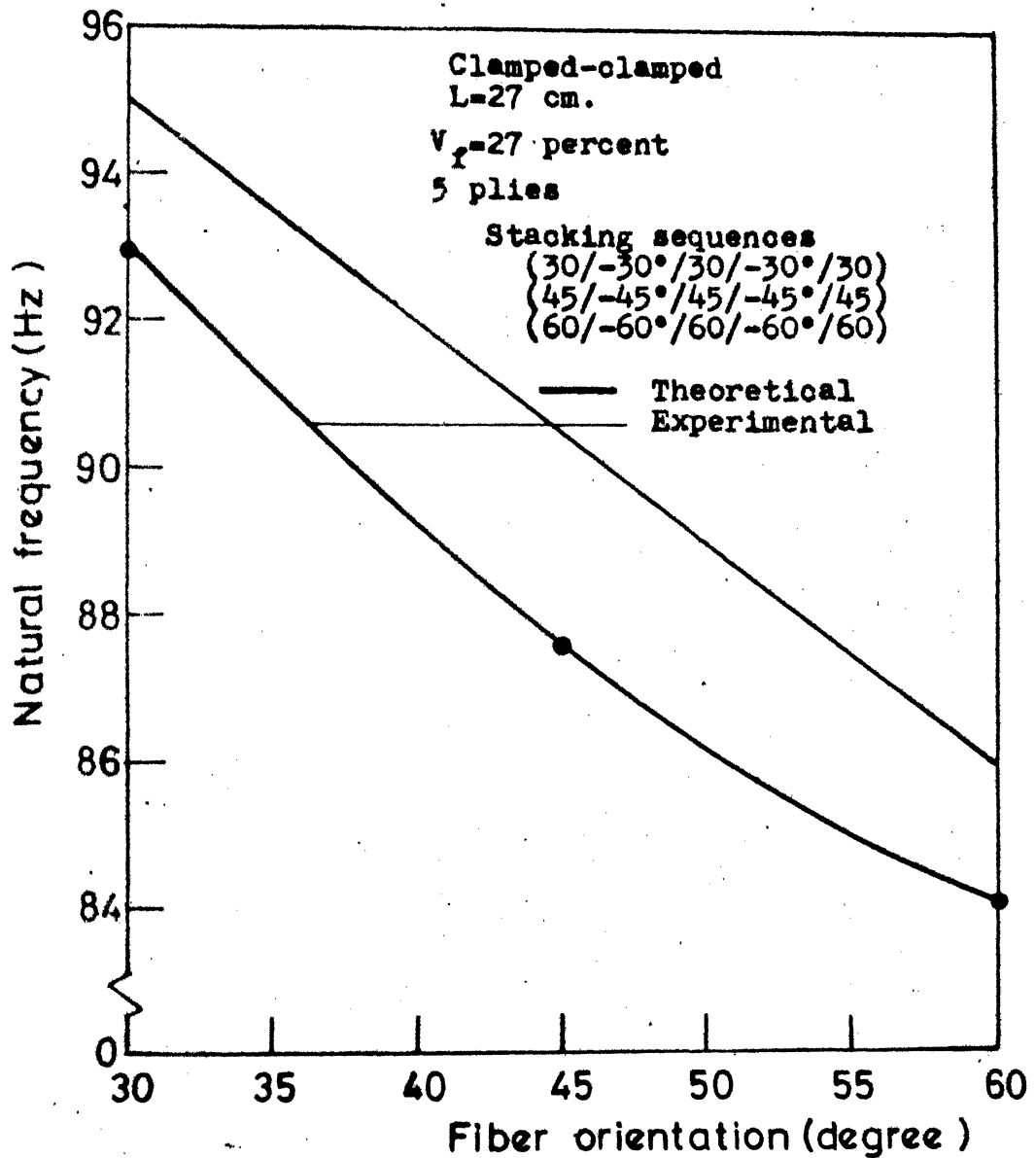
FIG. 4.2.5 VARIATION OF NATURAL FREQUENCY WITH FIBER ORIENTATION
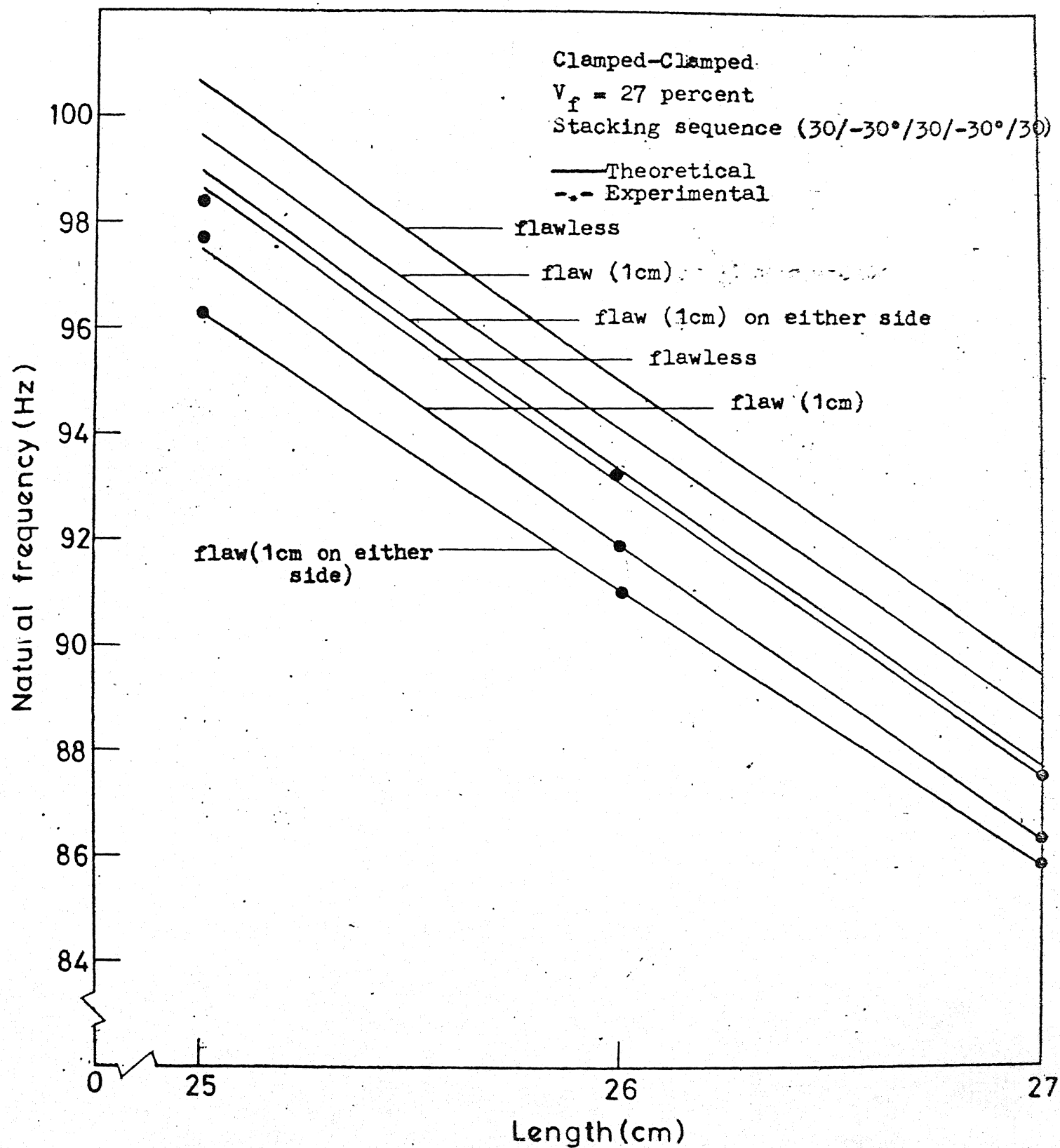
FIG. 4.2.6 VARIATION OF NATURAL FREQUENCY WITH LENGTH

FIG. 4.2.7 VARIATION OF NATURAL FREQUENCY WITH LENGTH

Clamped - clamped
V_f = 27 percent
Stacking sequence (0/45/90/45/0)
—Theoretical
-.- Experimental
flawless
flaw (1cm)
flawless
flaw (1cm on either side)
flaw (1cm)
flaw (2cm)
flaw (1 cm on either side)
flaw (2 cm on either side)
flaw (2cm)
flaw(2 cm on either side)
106
104
102
100
98
96
94
92
Natural frequency (Hz)
0,25
26
27
Length (cm)

V_f = 27 percent
Stacking sequence (0/90°/0/90°/0)
— Theoretical
-.-Experimental
flawless
flaw(1cm)
flawless
flaw(1cm on either side)
flaw (1cm)
flaw (2cm)
flaw (2cm)
flaw(1 cm on either side)
flaw(2 cm on either side)
flaw(2 cm on either side)
119
115
111
107
0,25
26
27
27.4
Length (cm)
Natural frequency (Hz)

FIG. 4.2.10 VARIATION OF NATURAL FREQUENCY WITH AREA OF FLAW
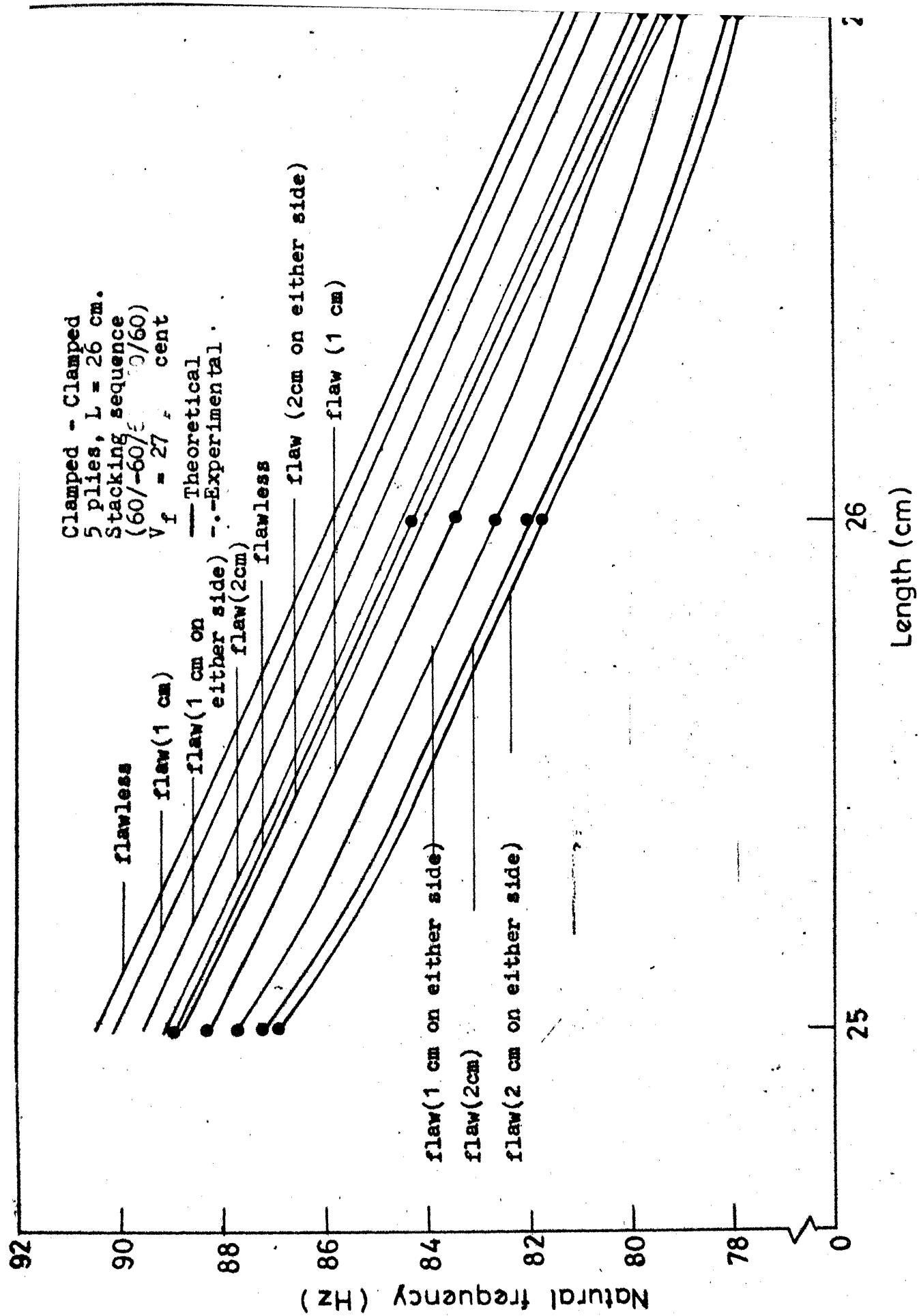
FIG 4.2.11 VARIATION OF NATURAL FREQUENCY WITH LENGTH
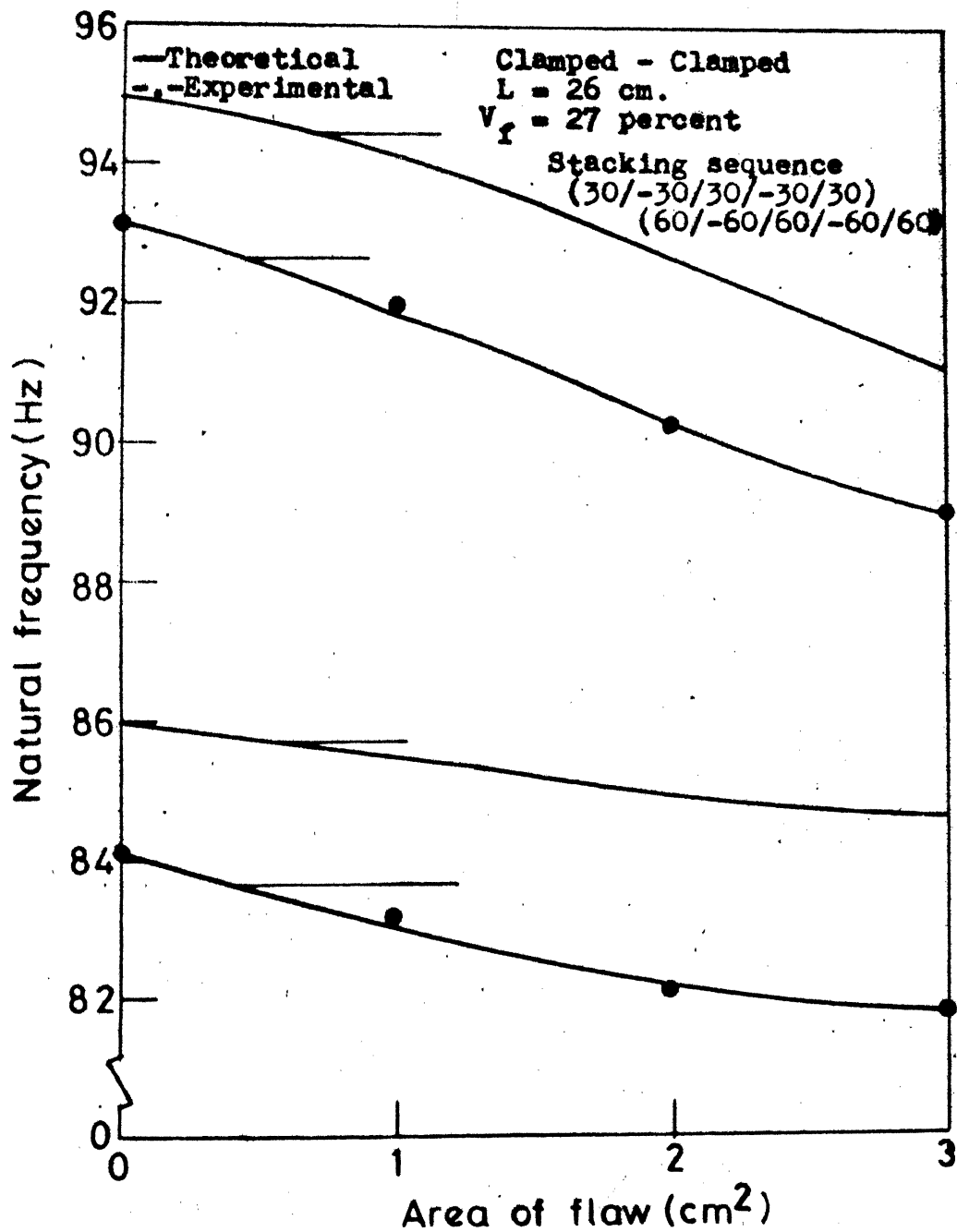
FIG. 4.2.12 VARIATION OF NATURAL FREQUENCY WITH AREA OF FLAW
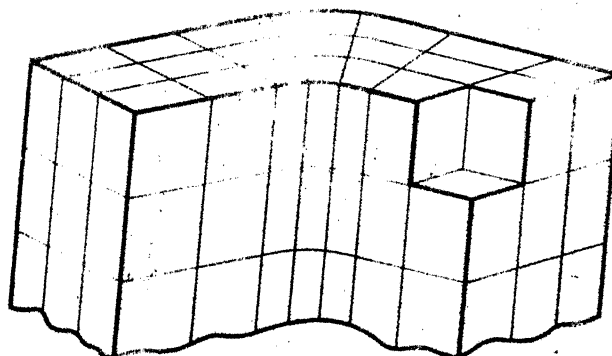
Fig 2:1. A systematic way of dividing a three dimensional object into "brick"-type elements

(a)
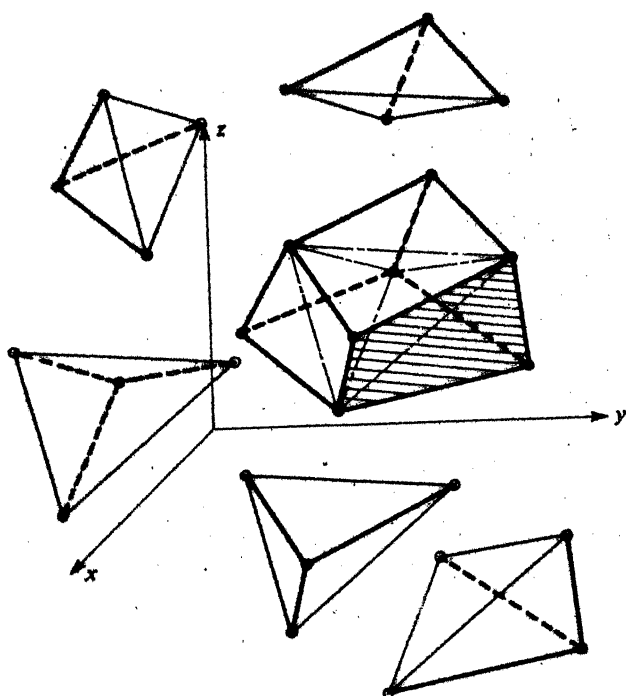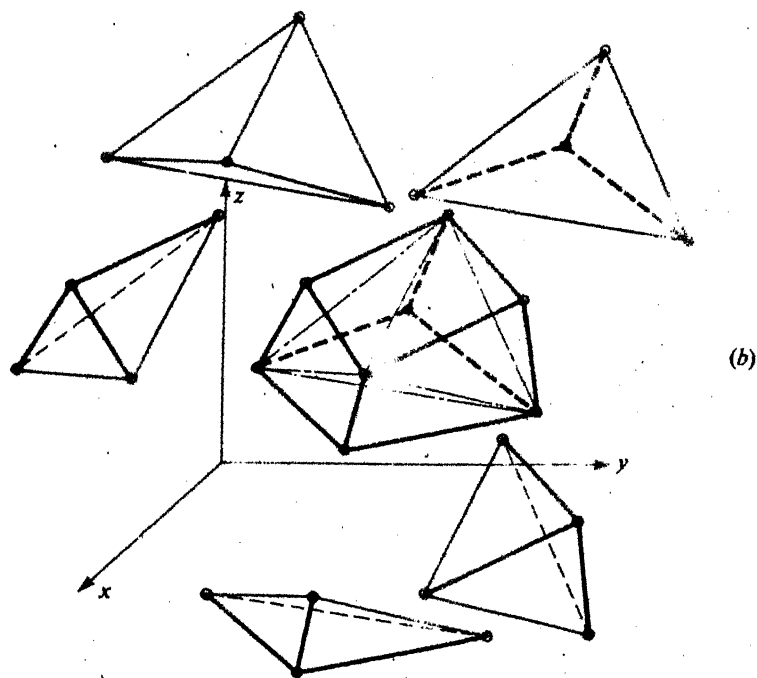
Fig. 2.12 Composite element with eight nodes and its subdivision into five tetrahedra by alternatives (*a*) or (*b*)
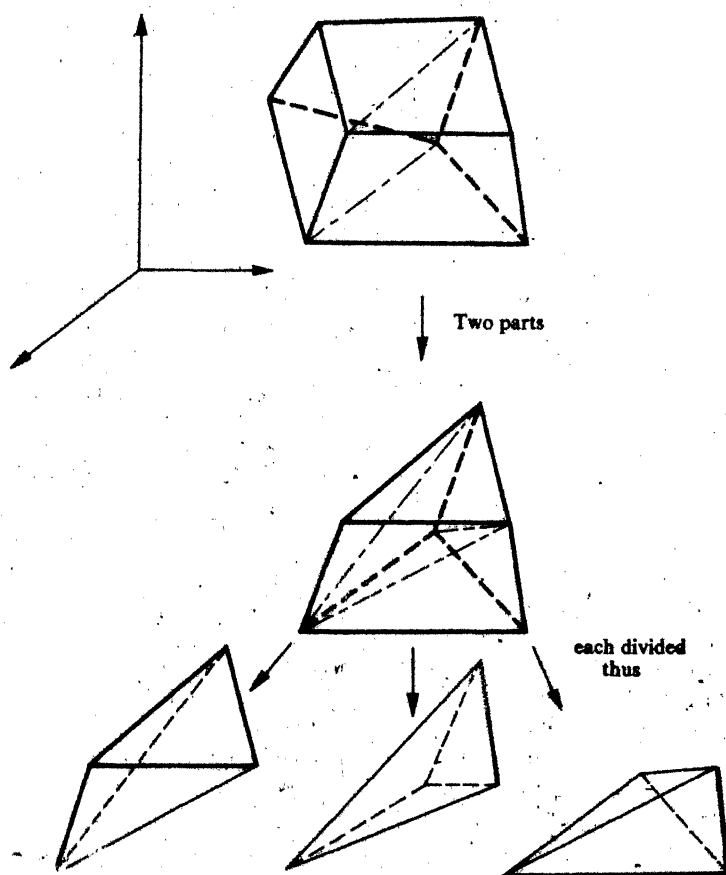
Fig. 2.3A systematic way of splitting an eight-cornered brick into six tetrahedra
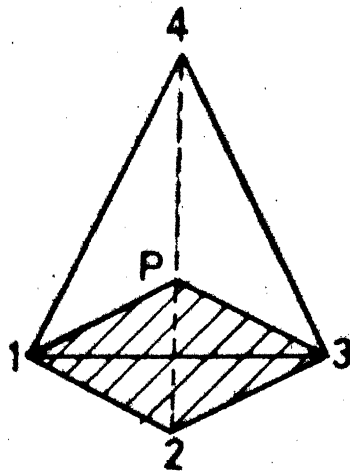
FIG. 2.4
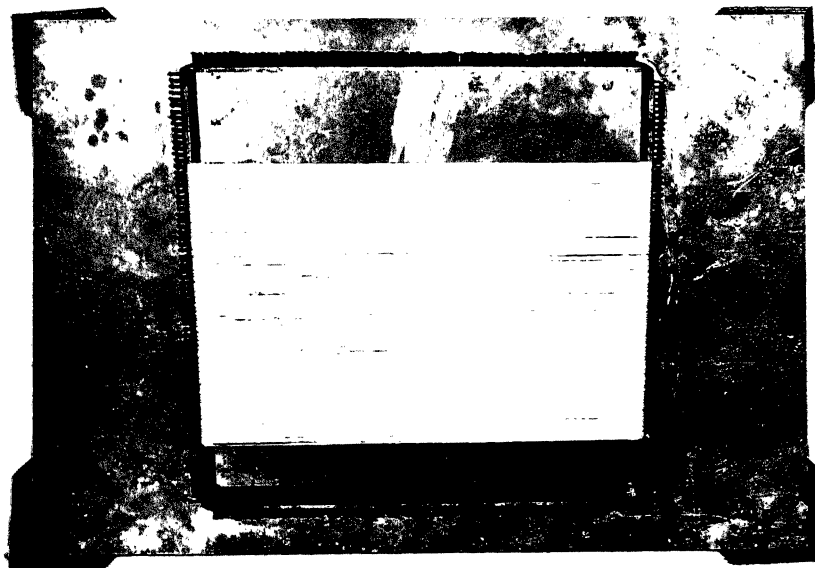
Fig. 3.1 WINDING FRAME WITH FIBERS
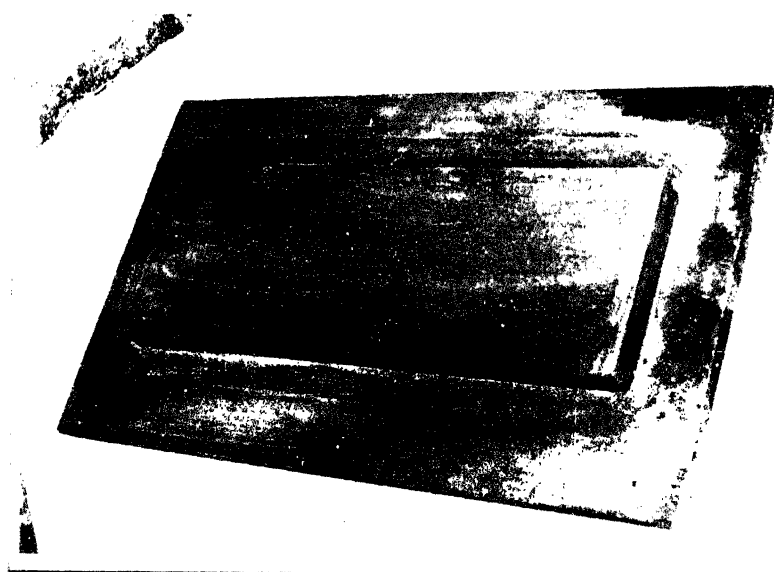
Fig. 3.2a & b DIE
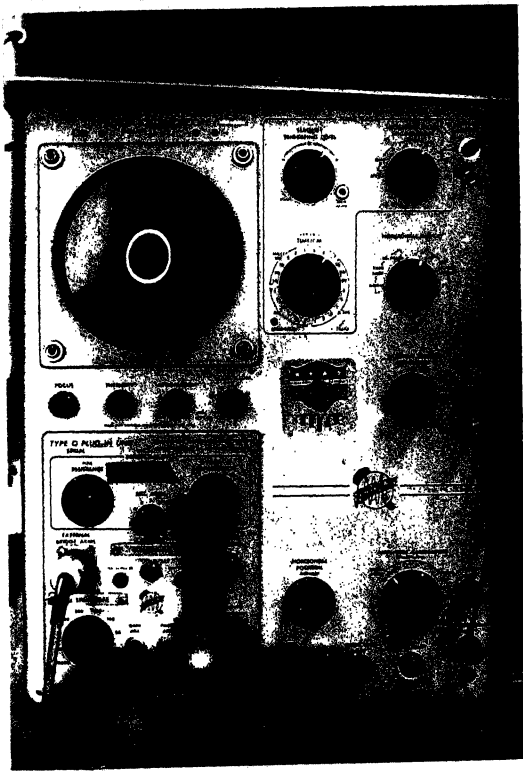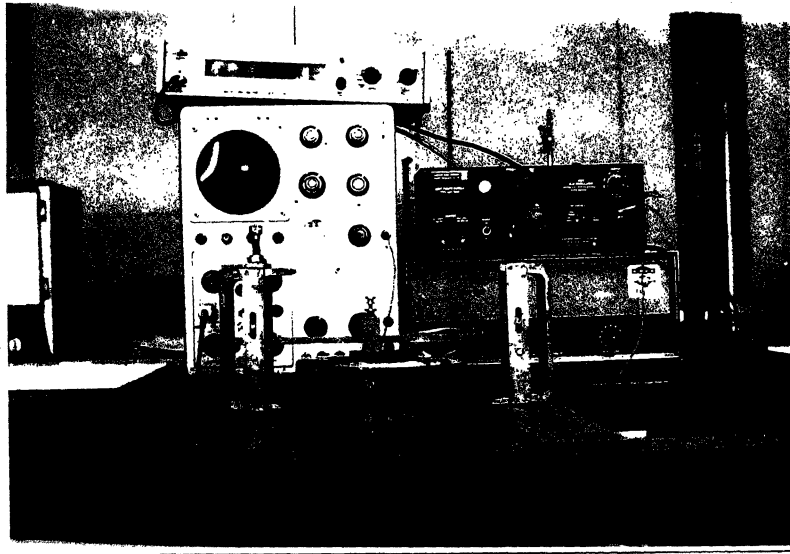
Fig. 3.3 EXPERIMENTAL SET UP

APPENDIX

Equation (18) shows the elasticity matrix for an element.

$$[K]^{(e)} = \int_V [B]^T [D][B]\, dV$$

where

$$[D]^{(e)} = [T]^{-1} [Q][T] = [\bar{Q}]\ \theta$$

For 3-dimensional element, the Q matrix is given by

$$Q = \begin{bmatrix} Q_{11} & Q_{12} & Q_{13} & 0 & 0 & 0 \\ Q_{12} & Q_{22} & Q_{23} & 0 & 0 & 0 \\ Q_{13} & Q_{23} & Q_{33} & 0 & 0 & 0 \\ 0 & 0 & 0 & Q_{44} & 0 & 0 \\ 0 & 0 & 0 & 0 & Q_{55} & 0 \\ 0 & 0 & 0 & 0 & 0 & Q_{66} \end{bmatrix}$$

where

$$Q_{11} = \frac{1-\nu_{23}\nu_{32}}{E_2E_3\Delta}, \quad Q_{23} = \frac{\nu_{23}+\nu_{21}\nu_{13}}{E_1E_2\Delta}$$

$$Q_{12} = \frac{\nu_{21}+\nu_{31}\nu_{23}}{E_2E_3\Delta}, \quad Q_{33} = \frac{1-\nu_{12}\nu_{21}}{E_1E_2\Delta}$$

$$Q_{13} = \frac{\nu_{31}+\nu_{21}\nu_{32}}{E_2E_3\Delta}, \quad Q_{44} = G_{23}$$

$$Q_{22} = \frac{1-\nu_{31}\nu_{13}}{E_1E_3\Delta}, \quad Q_{55} = G_{31}, \quad Q_{66} = G_{12}$$

where $= \det = \dfrac{1-\nu_{12}\nu_{21}-\nu_{23}\nu_{32}-\nu_{31}\nu_{13}-2\nu_{21}\nu_{32}\nu_{1}}{E_1E_2E_3}$

And also $\dfrac{\nu_{ij}}{E_i} = \dfrac{\nu_{ji}}{E_j}$

$$[m]^e = \omega^2 \int_{vol.} \rho \, [N]^T [N] \, dV$$

where

$$[N] = \begin{bmatrix} L_1 & 0 & 0 & L_2 & 0 & 0 & L_3 & 0 & 0 & L_4 & 0 & 0 \\ 0 & L_1 & 0 & 0 & L_2 & 0 & 0 & L_3 & 0 & 0 & L_4 & 0 \\ 0 & 0 & L_1 & 0 & 0 & L_2 & 0 & 0 & L_3 & 0 & 0 & L_4 \end{bmatrix}$$

and

$$[N]^T [N] = \begin{bmatrix} L_1^2 & 0 & 0 & L_1L_2 & 0 & 0 & L_1L_3 & 0 & 0 & L_1L_4 & 0 & 0 \\ 0 & L_1^2 & 0 & 0 & L_1L_2 & 0 & 0 & L_1L_3 & 0 & 0 & L_1L_4 & 0 \\ 0 & 0 & L_1^2 & 0 & 0 & L_1L_2 & 0 & 0 & L_1L_3 & 0 & 0 & L_1 \\ L_1L_2 & 0 & 0 & L_2^2 & 0 & 0 & L_2L_3 & 0 & 0 & L_2L_4 & 0 & 0 \\ 0 & L_1L_2 & 0 & 0 & L_2^2 & 0 & 0 & L_2L_3 & 0 & 0 & L_2L_4 & 0 \\ 0 & 0 & L_1L_2 & 0 & 0 & L_2^2 & 0 & 0 & L_2L_3 & 0 & 0 & L_2I \\ L_1L_3 & 0 & 0 & L_2L_3 & 0 & 0 & L_3^2 & 0 & 0 & L_3L_4 & 0 & 0 \\ 0 & L_1L_3 & 0 & 0 & L_2L_3 & 0 & 0 & L_3^2 & 0 & 0 & L_3L_4 & 0 \\ 0 & 0 & L_1L_3 & 0 & 0 & L_2L_3 & 0 & 0 & L_3^2 & 0 & 0 & L_3L \\ L_1L_4 & 0 & 0 & L_2L_4 & 0 & 0 & L_3L_4 & 0 & 0 & L_4^2 & 0 & 0 \\ 0 & L_1L_4 & 0 & 0 & L_2L_4 & 0 & 0 & L_3L_4 & 0 & 0 & L_4^2 & 0 \\ 0 & 0 & L_1L_4 & 0 & 0 & L_2L_4 & 0 & 0 & L_3L_4 & 0 & 0 & L_4^2 \end{bmatrix}$$

using

$$\iiint_V L_1^a \, L_2^b \, L_3^c \, L_4^d \, dV = \frac{a!\,b!\,c!\,d!}{(a+b+c+d+3)!} \, 6V$$

and integrating it we get the element mass matrix $[m]^e$

with $\rho V = W$

$$[M]^{(e)} = \frac{W}{10}\left[\begin{array}{ccc|ccc|ccc|ccc}
1 & 0 & 0 & \frac{1}{2} & 0 & 0 & \frac{1}{2} & 0 & 0 & \frac{1}{2} & 0 & 0 \\
0 & 1 & 0 & 0 & \frac{1}{2} & 0 & 0 & \frac{1}{2} & 0 & 0 & \frac{1}{2} & 0 \\
0 & 0 & 1 & 0 & 0 & \frac{1}{2} & 0 & 0 & \frac{1}{2} & 0 & 0 & \frac{1}{2} \\
\hline
\frac{1}{2} & 0 & 0 & 1 & 0 & 0 & \frac{1}{2} & 0 & 0 & \frac{1}{2} & 0 & 0 \\
0 & \frac{1}{2} & 0 & 0 & 1 & 0 & 0 & \frac{1}{2} & 0 & 0 & \frac{1}{2} & 0 \\
0 & 0 & \frac{1}{2} & 0 & 0 & 1 & 0 & 0 & \frac{1}{2} & 0 & 0 & \frac{1}{2} \\
\hline
\frac{1}{2} & 0 & 0 & \frac{1}{2} & 0 & 0 & 1 & 0 & 0 & \frac{1}{2} & 0 & 0 \\
0 & \frac{1}{2} & 0 & 0 & \frac{1}{2} & 0 & 0 & 1 & 0 & 0 & \frac{1}{2} & 0 \\
0 & 0 & \frac{1}{2} & 0 & 0 & \frac{1}{2} & 0 & 0 & 1 & 0 & 0 & \frac{1}{2} \\
\hline
\frac{1}{2} & 0 & 0 & \frac{1}{2} & 0 & 0 & \frac{1}{2} & 0 & 0 & 1 & 0 & 0 \\
0 & \frac{1}{2} & 0 & 0 & \frac{1}{2} & 0 & 0 & \frac{1}{2} & 0 & 0 & 1 & 0 \\
0 & 0 & \frac{1}{2} & 0 & 0 & \frac{1}{2} & 0 & 0 & \frac{1}{2} & 0 & 0 & 1
\end{array}\right]$$

and consistent mass matrix becomes

$$[M] = [T]^T [M]^{(e)} \quad [T]$$

where

$[T]$ is transformation matrix given by :

$$T = \begin{bmatrix}
\cos^2\theta & \sin^2\theta & 0 & 0 & 0 & 2\sin\theta\cos\theta \\
\sin^2\theta & \cos^2\theta & 0 & 0 & 0 & -2\sin\theta\cos\theta \\
0 & 0 & 1 & 0 & 0 & 0 \\
0 & 0 & 0 & \cos\theta & -\sin\theta & 0 \\
0 & 0 & 0 & \sin\theta & \cos\theta & 0 \\
-\cos\theta\sin\theta & \cos\theta\sin\theta & 0 & 0 & 0 & \cos^2\theta-\sin^2\theta
\end{bmatrix}$$

REFERENCES

1. Application of the new hybrid material {ARALL}, 13th congress international council of the Aeronautical Society, Vol. 2, seattle, Washington, pp 990 (1982).

2. Composite structures repair, 13th congress international council of the Aeronautical Society, Vol. 2, seattle, Washington, pp. 1386 (1982).

3. Kulkarani S.V. and Daniel Frederick. Frequency as a parameter in Delamination problem-A Preliminary investigation, J. of composite materials, vol. 5, pp. 112-117 (1981).

4. Daniel I.M., Mech. of Mater. Div., I.I.T. Res. Inst., Chicago, Behaviour of graphite/epoxy plates with holes under biaxial loading, Experimental Mechanics 20, 1, 1-8(1980)

5. Stepanenko, N.D. and et al. Rational bonding of structures from composite materials, Soviet Physics Doklady, pp. 907-909 (1978).

6. Harris, A., and Orringer, O., Investigation of angle ply delamination specimen for interlaminar strength test, J. of composite materials, 12, pp 285-289 (1978)

7. Chawla K.K., Inst. Milde, cung., Nucleation and propogation of fatigue creacks in A1-304 stainless steel laminate composite, J. of Materials Science, 14, 9, 2143-2150(1979).

8. Glavotto et al.
Anisotropic beam theory and applications, J. of Computer Structure, vol. 16, 1-4 pp 403-413 (1983).

9. Tirosh, J., et al.
The role of fibrous reinforcement well bonded or partially debonded on the transverse strength of composite materials, Engineering Fracture Mechanics, 12, 2, 267-277 (1979).

10. Ahmed K.M.
Free vibration of curved sandwitch beams by the method of finite element, J. of sound & vibration, 18, pp 61-74(1972)

11. Gajbir Singh
Vibration of laminated composite beams with flaws, M.Tech. Thesis, IIT Kanpur (1982).

12. Venkateswara Rao
Finite element analysis of vibration and stability problems, Ph.D. Thesis, II Sc., Bangalore (1972).

13. Jennings A. & R.B. Corr
A simultaneous iteration algorithm for symmetric eigen value Problem, Int. J. Num. Methods in Engg., vol. 10, pp 647-663 (1976).

14. Herakovitch C.T.
An optimal design of simple symmetric laminate, J. of Composite Material, vol. 15 (1981).

15. Meyer C.

Solution of equation of state of the art, J. of structure div., ASCE 99, 7 pp 1507-26 (1973).

16. Meyer C.

Special problem related to linear equation, J. of structure div., ASCE, 101, 4, pp 869-90 (1975).

17. Zienkiewicz, O.C.

The Finite Element Method, McGraw Hill Book Co., New Delhi, 1979.